Document Number	ESS-0060903
Date	January 15, 2019
Revision	4
State	Draft
Confidenitiality Level	Internal

Requirements and Technical Specifications - ESS nBLM System

	Name	Role/Title
Owner	Irena Dolen Kittelmann	Scientist / BLM system lead
Reviewer		
Approver		

Contents

1 Introduction

One of the proton beam instrumentation systems to be operated at the ESS linac is the Beam Loss Monitoring (BLM) system. Its primary goal is to detect abnormal beam behaviour and promptly inhibit beam production in case of beam failures in order to keep the machine safe from beam-induced damage. In addition to the protection functionality, the system is expected to provide the means to monitor the beam losses during normal operation with the aim to avoid excessive machine activation.

The ESS BLM system is divided in 3 sub–systems based on the detector technology:

- Ionisation Chamber based BLM (icBLM),
- Advanced BLM (cBLM),
- Neutron sensitive BLM (nBLM).

The first two BLM types mentioned above are based on charged particle detection and will be primarily located in the superconducting (SC) sections of the ESS linac. However, the expected particle fields outside the tanks in the normal conducting (NC) parts of the ESS linac are expected to be dominated by neutrons and photons. Thus, neutron sensitive detectors are needed in these sections.

Another issue to consider is the photon background due to the RF cavities. This is mainly due to field emission from the electrons form the cavity walls, resulting in bremsstrahlung photons created on the cavities or the beam pipe materials[1].

The nBLM system is based on Micromegas detectors designed to be sensitive to fast neutrons and insensitive to low energy photons (X– and –rays). In addition to this, the detectors are partly or fully (depending on the detector type) insensitive to thermal neutrons since part of these is not expected to be directly correlated to the fast beam losses.

This document states requirements and describes technical specifications for the nBLM system.

2 nBLM system

2.1 Level4 requirements

Table 1 gives a snapshot from the Level4 (L4) Proton Beam Instrumentation (PBI) requirements [2] relevant for the BLM systems, which were set in the past.

#	Type	Name	Description
1	Beam loss	XXX beam loss measurement	The beam loss shall be measured in the XXX section.
2	Beam loss	XXX beam loss measurement sensitivity	A beam current loss of 10 mW/m shall be detected.
3	General	XXX PBI damaging beam detection mitigation	Beam conditions that are potentially damaging to machine components shall be detected by the instrumentation and reported fast enough so that the conditions can be mitigated before damage occurs.
4	General	XXX PBI peak current range	Proton beam instrumentation in the XXX section shall function over a peak beam current range of 3 mA to 65 mA.
5	General	XXX PBI pulse length range.	Proton beam instrumentation in the XXX section shall function over a proton beam pulse length range of 5 µs to 2.980 ms.
6	General	XXX PBI pulse-by pulse measurement update rate	Unless specifically stated, all instrumentation shall be able to perform the measurements and report the relevant PV data at a repetition rate of 14 Hz.

Table 1: L4 PBI requirements [2] relevant for the BLM system. The 'XXX' refers to specific linac section and runs over all section from including MEBT on.

2.2 Requirements on the components

The following has been required for the BLM system components:

1. Any BLM system hardware component shall be compatible with the radiation environment specific to the component location.

2. All components of the system (detector, electronics, mechanical support, software, firmware, etc) shall be compliant with the standards set by ESS ERIC. In particular, the firmware

design and implementation shall follow the FPGA Development Standards available in [4].

3. The same Fast Beam Interlock System (FBIS) interface card shall be used for all BLM systems.

2.3 Response time of the system (requirement)

The time response of the system is defined as the time from the onset of the beam loss to the time when the decision about unacceptable conditions reaches the output connector on the BLM side leading to the Fast Beam Interlock System (FBIS) interface card.

Currently the Machine Protection System (MPS) requires the BLM system to react within 10 µs in the Superconducting (SC) and within 5 µs in the Normal Conducting (NC) parts of the ESS linac [3], the latter being applicable to the nBLM system. However, these numbers were set in the past based on a simplified calculation of time needed to melt a block of material under a perpendicular incidence and for the beam parameters before [5] and after [6] the linac redesign in 2014.

2.4 Mode of operation

The nBLM system is designed to operate in two modes, where the transition between them is automatic:

- **Counting mode**: Individual neutron signals are detected and counted.
- **Current mode**: The rate of incoming neutrons is too high for the system to be able to distinguish between two individual neutron signals, hence events pile up. In this case the number of neutrons is estimated through the charge.

2.5 Components overview

Each nBLM detector is enclosed in a detector module box together with a custom made Front-End Electronics (FEE). Analogue signal from each nBLM detector module located in the ESS tunnel are routed through a coaxial cable to the klystron gallery, where it connects to the Back-End Electronics (BEE). Here the signal is first digitised and sampled at 250 MS/s rate by a DC coupled 8 channel ADC (IOxOS ADC3111 FMC board [7]). The signal is then processed by a μTCA based IOxOS IFC1410 AMC board equipped with an FPGA [8]. The board includes a CPU as well, however a Single Board Computer (SBC) has been selected instead of the embedded CPU for the final nBLM design. The choice is consistent with the design of nBLM and other beam diagnostics systems. The main role of SBC is to provide an interface to the ESS control system. The SBC type is compliant with the ESS standards. Similarly, an ESS standard timing module (Event Receiver – EVR) is used to interface the ESS timing system.

Signal cables running from the tunnel to the klystron gallery are enclosed in cable conduits for additional shielding. It is planed to have each conduit housing signal cables from several different systems (icBLM, nBLM, BCM). The work on requirements and design of signal cables is ongoing.

Both high and low voltage power supply modules are located in the same crates, namely CAEN SY4572 [9]. Two crates are foreseen to allow controlling and monitoring of the high and low voltage power supplies. The 48–channel CAEN A7030 modules [10] provide high voltage to the mesh (–400 V to –500 V towards anode) and the drift (–500 V to –1000 V towards mesh) of each Micromegas detector in independent lines. Similarly, the CAEN A2519 modules [11] are used to power several groups of FEE cards. The module provides ± 5 and 0 V to each detector FEE. Detailed schematic of connections between LV card and detectors is given in reference [36].

To ensure a stable operation on a time scale of years the nBLM chambers need a continues flow of gas at the level of 0.1 l/h. A PLC with Siemens S7-1500 [12] controller is used for controlling and monitoring of the gas flow. Further details about the hardware components selected for the controlling and monitoring the gas system are given in reference [36].

Full hardware overview of the nBLM system for one detector module is given on figure 1. Further details and overall connection and grounding scheme is given in reference [43].

2.5.1 FBIS interface and Low Latency Link connection

A piggyback card providing a set of electrical interfaces to the ESS Machine Protection Fast Beam Interlock System (MPS FBIS) has been foreseen. The card may either be used through an FMC or RTM card [18] that can be paired with the IFC1410 platform.

All BLM subsystems are required to use the same FBIS hardware interface options and be able to process up to 8 detector channels. The IFC1410 card has two FMC slots available. In case of nBLM, only one FMC slot is occupied (with 8-channel ADC3111) and the other one can be used for the FBIS interface. However, in case of icBLM, the RTM solution is the only available choice if the pico4 card (4 channels) is selected as the acquisition unit, while both RTM and FMC solution are possible in case of BLEDP (8 channels) selection.

As the pico4 option has been chosen in the final design of the icBLM, the RTM based interface to FBIS has finally been selected. However the RTM card is currently still under development and is anticipated to be available only in September 2019. Therefore an intermediate solution based on a IOxOS DIO3118 DIO FMC [22] has been foreseen as an intermediate solution for test purposes, though this option does not fulfil the FBIS interface requirements. The interface document between BLM systems and FBIS is available in reference [44]. The exact definition of all signals exchanged with the FBIS is not finalised and is under discussion with Machine Protection (MP) team.

An option to combine the data originating from different processing units is foreseen for the future upgrade. This can among other things enable identification of coincident signals between two different BLM channels that are not processed by the same BEE card or even between a BLM channel and certain condition on a BCM channel. The approach requires a functioning

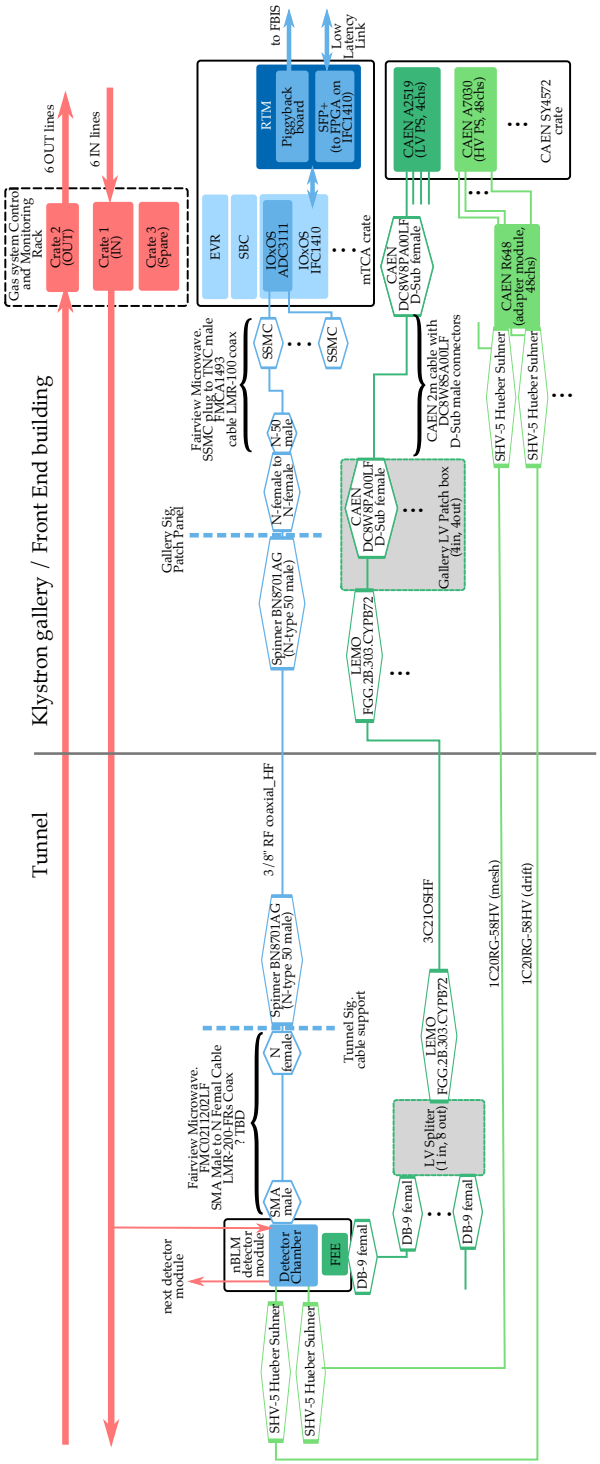

Figure 1: Schematic overview of the nBLM system for one detector module. Further details related to LV connections, cable supports on the detector side and gas system control and monitoring components are available in [36].

Low Latency Link (LLL). At least one SFP+ connection to the FPGA has been foreseen to be provided through the above mentioned RTM card. In case of nBLM and icBLM systems the connection is planned to be used for LLL communication.

3 Detectors

This chapter gives an overview of the requirements and specifications relevant for the design of the nBLM detectors in addition to the ones already specified in section 2. A short description of the final detector design and references with details are presented here as well.

3.1 Requirements and specifications

3.1.1 Expected particle fluxes and spectra

The nBLM system is the primary beam loss monitor in the NC line (MEBT, DTL). Preliminary studies based on Monte-Carlo (MC) simulations of lost protons for various loss scenarios along the DTL part of the ESS linac have been performed [15].

The background is mainly due to the RF induced low energy photons (X– and γ–rays). Additionally, low energy neutrons that are not related to the prompt beam loss can be expected. The latter can be estimated through MC simulations of lost protons along the linac, however special care must be taken due to the focus on the thermal neutrons. Rough estimations are available in results from studies in [15, 16].

The levels of the photon background cannot be predicted numerically since they depend on time as well as operation conditions and quality of the cavities. On the other hand energy spectra can be estimated due to the known physical process involved in production of this background (bremsstrahlung). Nevertheless, this background is planned to be assessed experimentally in environments as close as possible to the ESS linac. This can be done IN CERN at LINAC4 which consist of a DTL similar to the ESS DTL or at test stands with the ESS SC cavities.

3.1.2 Neutron energy limit

An estimation on the energy limit that separates between the fast and slow neutrons was needed to optimise the detector design for the ESS linac. Preliminary studies in the DTL parts of the linac [15] gave an upper (0.5 MeV) and lower limit (0.05 MeV) on this value that ensure acceptable purity and detector efficiency. See the reference for details.

3.1.3 Dynamic range

The lower and upper limit of the dynamic range for the system are set by the L4 PBI requirements #2 and #3 from table 1. The values in terms of detected particles or detected signal can be estimated through MC simulations of lost protons and depend on detector location. In the case of upper limit they depend on beam parameters and accidental loss scenarios as well. However due to large number of possible accidental scenarios and lack of their time dependent loss maps, some simplifications and assumptions must be made. A strategy of how this is handled is given in [16, 15].

Preliminary studies based on MC simulations of lost protons for various loss scenarios along the DTL part of the ESS linac [15, 16] gave a general view of expected neutron rates along the DTL. These studies then served as an input to further MC simulations focused on the detector performance aiming to tune the detector design to the ESS linac conditions. Estimations on the expected detector signals and rates for various loss scenarios can be found in report of these studies [17, 18, 19, 20].

3.2 Design

3.2.1 Detector chamber

Micromegas detectors [26, 27] were chosen for the nBLM system. They are designed to be sensitive to fast neutrons while insensitive to the low energy photons (X– and γ–rays) in order to suppress the RF induced photon background contribution to the signal. Additionally, the signals from thermal neutrons are suppressed as they may not be directly correlated to the beam losses.

A Micromegas is a parallel plate gas detector with three electrodes: cathode (drift electrode), micromesh and anode. Micromesh, which is held by insulating pillars at a small distance (0.1 mm) from the anode, divides the detector chamber in two regions: the drift region towards the cathode and amplification region towards the anode (see figure 2).

Incoming charged particles ionise the gas in detector. The electrons produced through ioni-

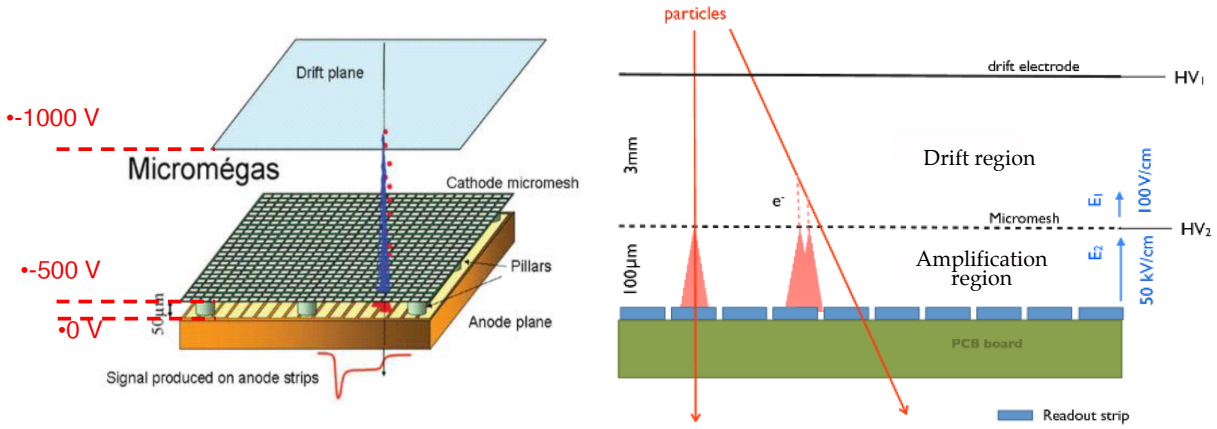

Figure 2: Schematic view of a micromegas detector.

sation process, drift towards the mesh under the influence of the electric filed applied to the drift region (typically 10^2 V/cm to 10^3 V/cm). Stronger electric field in the amplification region 10^4 V/cm to 10^5 V/cm) guides the electrons through the holes in the mesh to the amplification region. Here the electron multiplication occurs producing an avalanche which amplifies the resulting negative signal, read out on the anode side.

Typical signal produced in such a detector is of few mV with a current of few µA. The rise time

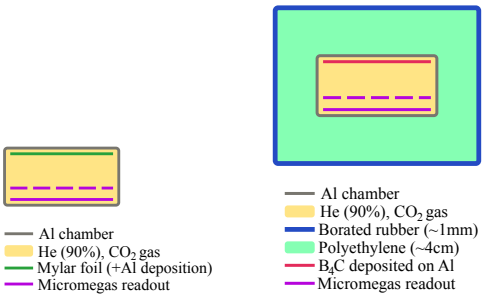

Figure 3: Schematic view of a nBLM-F (left) and nBLM-F (right) detector.

is in general 30 ns to 50 ns while the pulse duration 100 ns to 200 ns. Both can be tuned with the length of the drift region (drift distance). Note that a micromegas detector in its typical form detects charged particles and needs a converter material to transform neutrons to charged particles which can be detected.

Two different types of nBLM detectors with complementary functionality will be installed along the ESS linac:

- Fast detectors (nBLM-F): aimed to detect fast losses when high particle fluxes are expected (accidental beam losses).
- Slow detectors (nBLM-S): primarily aimed to monitor slow losses when low particle fluxes are expected.

A common design of the detector chamber has been adopted for both detector types. The only difference is in the cathode due to the different conversion material used in each of the detector types. The chamber dimensions are $15\,\mathrm{cm}^3 \times 25\,\mathrm{cm}^3 \times 5\,\mathrm{cm}^3$, while in the case of the slow detector together with the moderator the overall dimension amounts to $25\,\mathrm{cm}^3 \times 25\,\mathrm{cm}^3 \times 15\,\mathrm{cm}^3$. The detector active area of $8\,\mathrm{cm}^2 \times 8\,\mathrm{cm}^2$ is segmented in 4 strips, that can be read independently or as one. To minimise the amount of cables and BEE cards needed, the latter option has been chosen, though the former option gives a possibility to adapt to high rates if needed. The Micromegas is built with the standard bulk technique [23] and is filled with a gas mixture of He (90%) + CO_2. The aluminium plate ($10\,\mathrm{cm}^3 \times 10\,\mathrm{cm}^3 \times 0.4\,\mathrm{cm}^3$) with the neutron converter is placed at a distance of 2 mm from the mesh, defining the drift region. The distance between the mesh and anode is 128 µm.

The following two subsections give an overview of principle of operation and differences between slow and fast nBLM detectors. Schematic view of both detector types is shown on figure 3. Additional details of detector design through various stages of development are given in [17, 19, 24, 22].

3.2.1.1 nBLM–F

Detection of fast neutrons is performed with the use of hydrogen rich material which serves as a neutron to proton converter through neutron elastic scattering on hydrogen atoms. The scattered protons ionise the gas contained in the detector chamber resulting in a measurable signal.

This type of detector is intrinsically insensitive to low energy neutrons as only neutrons with high enough energy can produce recoils with significant range to enter the detector drift region ($E_n \geq 0.5$ MeV). The rejection of low energy photons is achieved through the fact that low energy photo-electrons produce significantly lower ionisation compared to the proton recoils resulting in considerably lower signal levels.

The emitted protons have a continuous spectrum, resulting in a signal amplitude spread over a certain range. The detector has a preferred direction for neutron detection, as it is sensitive primarily to the neutrons incoming from the front side with converter due to the preferred direction of the emitted protons with respect to the primary neutron. The neutron detection efficiency ranges between 10^{-5} to 10^{-3} for neutron energies between 0.5 MeV and 10 MeV, while the time response is of the order of ns.

Mylar is used as a converter material for the nBLM-F detectors. Thus, cathode is a 125 µm Mylar foil with aluminium deposit of 50 nm in order to apply the voltage. The foil is glued to a 4 mm aluminium plate for robustness.

3.2.1.2 nBLM–S

This type of neutron detector is based on material with high cross-section for (n,α) which serves as a converter (^{10}B in case of nBLM–S). The reaction produces α particle emitted with a fixed energy. There are two channels of decay:

- α with 1.4 MeV (94 %) or
- α with 1.8 MeV (6 %) and γ with 480 keV.

The produced α enters the detector chamber volume and ionises the gas resulting in a signal that can be measured. The gamma suppression is like in case of nBLM–F detector based on the difference in the ionisation between electrons and α-s.

In case of nBLM–S type, the detector chamber is surrounded by a neutron moderator to thermalise the incoming fast neutrons in order to increase the conversion efficiency at the converter. The thickness of the moderator on the side of the cathode and anode has been set to 5 cm. Additionally, a shield of 5 mm borated rubber is placed in the outermost part of the detector to suppress part of the incoming background thermal neutrons.

The detector has a 4π acceptance for neutrons. The efficiency is in general more or less constant over a larger energy range (from few eV to tens of MeV) and can be as high as few %. The signal amplitude of this detector type is almost constant due to the fixed energy of detected α-s. Fluctuations arise from different incoming particle angles and the fact that a detector has

a given energy resolution. However, the neutron moderation process delays a larger part of the events by times from some 10 ns to 200 µs.

In case of nBLM–S, the cathode consists of a 4 mm aluminium plate coated with $^{10}B_4C$. The coating thickness influences the efficiency and has been set to 1.5 µm in the final design. If unacceptably high rates are measured in real ESS environment, the cathode with thicker coating could later be replaced with one with thinner coating.

3.2.2 Detector module

The detector module consists of (figure 4):

- Detector gas chamber which encloses the detector cathode and PCB with the anode readout together with micromegas mesh.
- FEE mezzanine card for FEE together with the signal and LV connections needed to power the FEE. The card is attached to the detector PCB.
- HV mezzanine card for supplying HV to the detector (2 HV connections, one for the mesh and one for the cathode/drift). The card is attached to the detector PCB.
- Faraday cage made of 1.5 mm thick aluminium box which encloses the detector PCB board and both mezzanine cards.
- In case of nBLM-S, the gas chamber is surrounded by a moderator with absorber though the same gas chamber design is used for both nBLM-S and nBLM-F modules.

The FEE mezzanine card includes 2 FAMMAS current amplifiers (Fast Amplifier Module for Micromegas ApplicationS) [21], low voltage filters and two output driver buffers (i.e. high impedance inputs). The consumption of the card is less than 200 mW and allows the operation in both counting and current mode.

The detector module mechanical design has been finalised in July 2018 (Critical Design Review CDR2). Details regarding the module and part of the detector mechanics together with the results leading to these choices can be found in [22, 23, 41]. Details about the FE and HV mezzanine cards are available in [24, 25, 36]. A summary of various test performed with the detectors through various stages of the design phase are given in [42, 23].

3.3 Detector layout

Consistently with the goal of nBLM system as the primary loss monitor in the NC parts of the ESS linac, the majority of detectors are placed in the DTL section. Here the detectors are positioned at every ∼1/4 (∼1 m) of a DTL tank length, resulting in 8 detectors per tank and a pair at the end. The placement is consistent with the results in [15], where RMS values in the

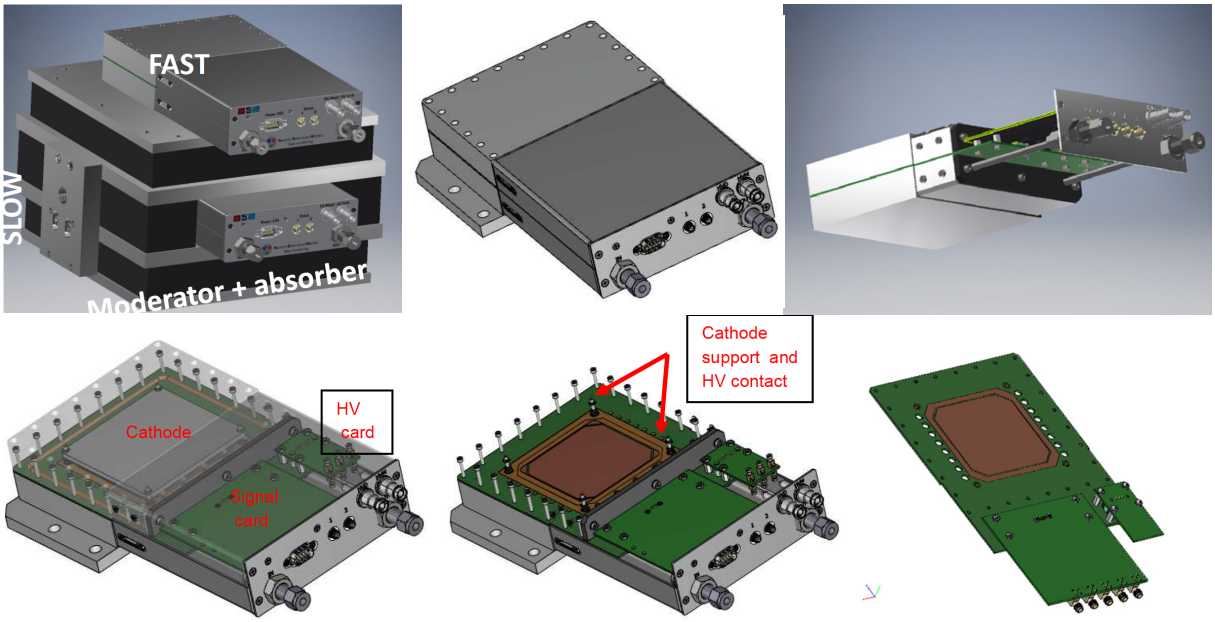

Figure 4: Top, left: fast (nBLM-F) and slow (nBLM-S) detector modules; middle: nBLM detector module with connectors visible on the closing face of the Faraday cage; right: same but with part of the Faraday cage open. Bottom, left: detector gas chamber and Faraday cage (transparent) with the mezzanine cards; middle: same but without the cathode to see the active surface of the Micromegas; right: detector PCB with the mezzanine cards.

distribution of particles 20 cm away from the tanks was found to vary between 0.9 m to 3.6 m for a set of scenarios of point losses in the DTL.

A significant number of detectors is located in the Spoke section following the DTL in order to make a smooth transition in coverage between nBLM as the primary monitor in the NC linac and icBLM in the SC linac. The arrangement also allows an option to compare the measurements between the two systems and potentially help to understand the background in terms of γ–particles and thermal neutrons. Other high energy parts of the linac are only sparsely populated with the nBLM detectors, where again their purpose is to help understand the background.

Majority of the nBLM detectors are placed in an alternating fashion by varying between nBLM-F and nBLM-S type along the linac. Though at certain positions a pair of both slow and fast detector is located. Alternating between fast and slow detectors is the case in the DTL section, with exception of a pair of detectors at the end of DTL. The same holds in Spoke section where one slow and one fast detector is placed at each cryomodule and Linac Warm Unit (LWU) respectively. On the other hand in other SC parts of the linac a pair of detectors is placed at few locations along the linac.

The full detector layout for the nBLM system is presented on figure 5 and summarised in table 2. Additionally, information about the icBLM detector locations is given as well.

Linac section	Num. of devices			
	icBLM		nBLM	
	comment	count	comment	count
MEBT		/		2F+2S=4
DTL	1/tank	5×1=5	8/tank,2/end	5×(4F+4S)+1F+1S=42
Σ		5		23F+23S=46
Spoke	1/cryo,3/2q	13×4=52	1/2q, 1/cryo	13×(F+S)=26
MB	1/cryo,3/2q	21×4=84		1F+1S=2
HB	1/cryo,3/2q	9×4=36		1F+1S=2
MEBT	3/2q	16×3=48		/
A2T				
ramp	1/bend,3/2q	6×3+2×1=20		1F+1S=2
to target	3/2q, 3/4rast.	3×3+2×3=15		2F+2S=4
dump	1/mag.	6		/
Σ		261		18F+18S=36
ΣΣ		266		41F+41S=82
ΣΣΣ				348

Table 2: icBLM and nBLM detector count in each of the ESS linac section. Here "q", "bend", "rast.", "mag." and "cryo" syand for quadrupole magnet pair, bend magnet, raster magner, magnet and cryo module.

3.4 Detector mounting

The space in the ESS 3D Plant Layout (EPL) has been claimed for all nBLM detectors and conceptual design of mechanical supports exist. However the work on mechanical integration of supports and detectors is ongoing with the exception of detectors in the DTL section, where the integration is finished.

The conceptual design for the support in MEBT is based on a foot attached to the floor (see figure 6). On the other hand, in the DTL section the detectors are mounted on holders attached to rails running along the DTL tanks as shown on figure 7.

In LWUs the same approach for nBLM detector mechanical supports has been adopted independent of the linac section. Here the detector supports are attached to the LWU supports and hold the detectors close to the beam line without extra material in the way. An example is given on figure 8.

Two options for the mechanical support of detectors located at Spoke cryomodule positions are available. The detectors can be either attached to the cryomodule through a metal band or attached to an aluminium profile hanging from the ceiling. The former option is planned as the baseline solution with the later as a backup.

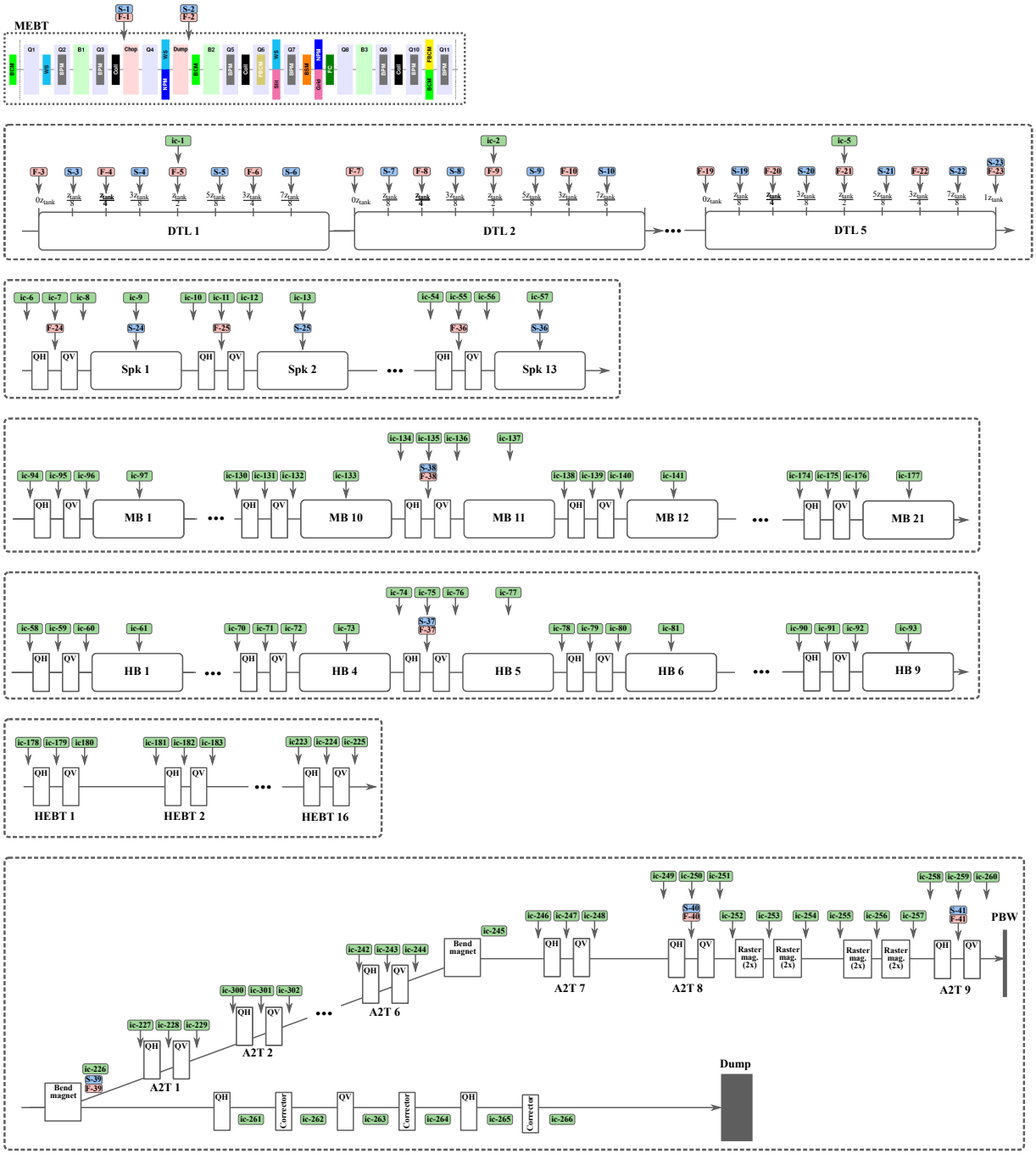

Figure 5: nBLM and icBLM detector layout along the ESS linac [28].

The design for all mechanical supports follows the same concept, where a holder is used to position the detector at certain angled from the vertical axis. The angle of 45° has been chosen as a baseline. Different angle and orientation around the beam line can be achieved by replacing the holder in case experience during the system commissioning indicate for baseline orientation to be inadequate. Further details regarding the mechanical support design are available in reference [36].

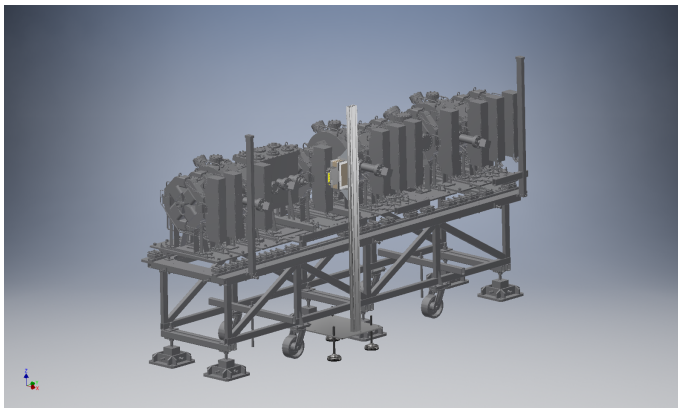

Figure 6: nBLM detector mounting in MEBT section.

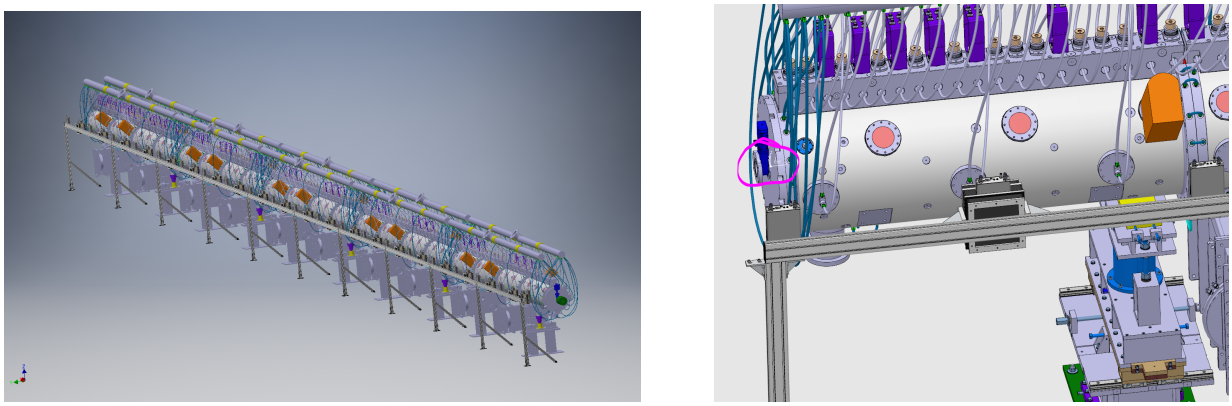

Figure 7: nBLM detector mounting in DTL section.

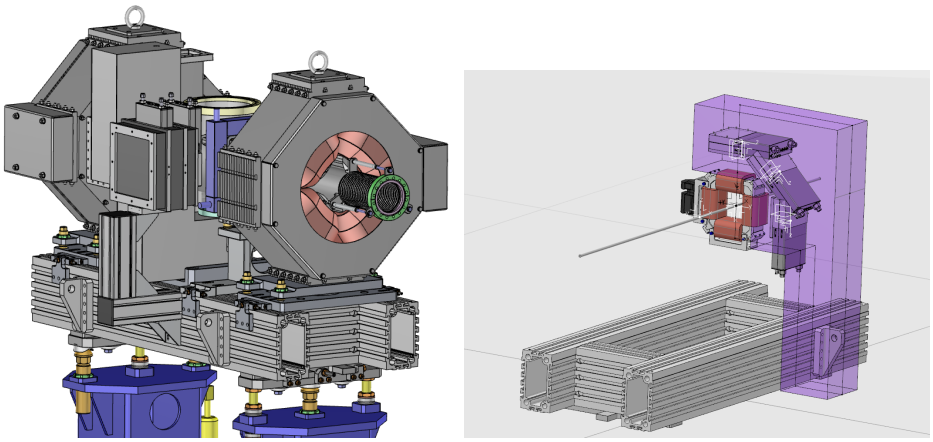

Figure 8: nBLM detector mounting in LWU4 of Medium Beta section (left) and 3 possible detector orientations (right).

4 Electronics layout

Each card, crate or rack is responsible for handling several detectors. In case one of these units experiences malfunction, the system may cease to be able to report beam losses over several subsections of the linac and in the worst case even fail to react on dangerous beam conditions. This poses a threat to the safety of the machine elements and if a larger part of the system becomes unavailable inhibiting beam production may be inevitable.

In order to avoid these situations and to increase the system availability, the detectors are collected in three groups. The first two groups cover linac sections from including MEBT to Spoke and are formed by grouping odd and even pairs of neighbouring fast and slow detectors. The two detector groups have all electronics related to the signal lines placed in separate racks, resulting in separation of signal connections between the two groups down to the rack level. The third group covers the rest of the detectors which are sparsely located in the high energy linac parts from including MB to A2T sections.

Signal cable layout is presented on figure 10 and summarised in table 3. The figure demonstrates the detector distribution among the racks and processing AMC cards along the linac. Slow and fast detectors are represented by triangles and circles respectively, while different colours are used to mark the grouping of detectors with green, red and blue indicating odd, even and high energy group respectively. Signal cables are routed through the nearest stub (yellow squares) to the racks marked with green, red or blue squares depending on which detector group they connect to. Different levels of circles and triangles along the vertical axis differentiate between the groups or sets of detectors connected to the same rack or AMC card respectively. Smaller difference between two detector sets in a group along the vertical axis distinguishes between different AMC cards in the same rack. Similarly, larger difference along the vertical axis between two collection of detectors in the same group distinguishes between two different racks the detectors connect to. Hence, the first 12 green detectors connect to the first green rack, while the following set of 12 green detectors connect to the second rack marked with green. On the other hand the first 3 green detectors connect to the first AMC in the first rack while the following 3 detectors connect to the second AMC card in the same rack.

Estimated signal cable lengths are presented on figure 9. The figure shows that signal cables are expected to be shorter than 100 m. Note that the routing through stubs used for these estimations is the same as indicated on figure 10.

Both HV and LV connections follow the same detector grouping as the signal connection. However only two crates are being deployed along the linac for both HV and LV PSs. In addition to this, each LV long haul cable is used to power several detectors. Thus, complete separation of LV or HV connections between the groups down to the rack level is not possible. Instead, care is taken that the same set of detector modules with signal cables connected to a particular AMC, has FEE powered by the same channel of a certain LV card (i.e. number of AMC cards equals number of LV channels in use). Similarly, the same set of detectors that has signal cables connected to a certain rack, has all HV cables connected to the same HV module.

HV and LV cabling is summarised in tables 4 and 5 respectively. Full overview of the system electronics layout is given on figure 11. Here the tag number of AMC card to which certain detector connects to is specified above the detector, where the colour indicates the group the detector belongs to. Different shades of the same colour are used to differentiate between the racks. Note also that the AMC card and LV channel tagging are equivalent. Additional, the tag number for both LV and HV card is shown above each detector as well.

Rack	Detector count	AMC count	Crate count	Detectors per AMC	AMC tag	Spare cables per rack
FEB-050ROW	24	4	2	(6+6),(6+6)	(1,3),(5,7)	2
SPK-010ROW	22	4	2	(6+6),(6+4)	(2,4),(6,8)	2
SPK-030ROW	14	3	1	(6+4+4)	(9,11,13)	2
SPK-050ROW	12	2	1	(6+6)	(10,12)	2
MBL-050ROW	2	1	1	(2)	(14)	4
HBL-090ROW	2	1	1	(2)	(15)	4
HEBT-030ROW	2	1	1	(2)	(16)	1
A2T-010ROW	4	1	1	(4)	(17)	1
Sum	**82**	**17**	**10**			**18**

Table 3: Summary of the nBLM system signal connections. The column marked with “Detectors per AMC” indicates the number of detectors connected to a crate or AMC board. The parenthesis "()” and "+” sign are used to differentiate between the crates and AMCs respectively. The colours mark different detector groups as explained in the text and shown on figure 10.

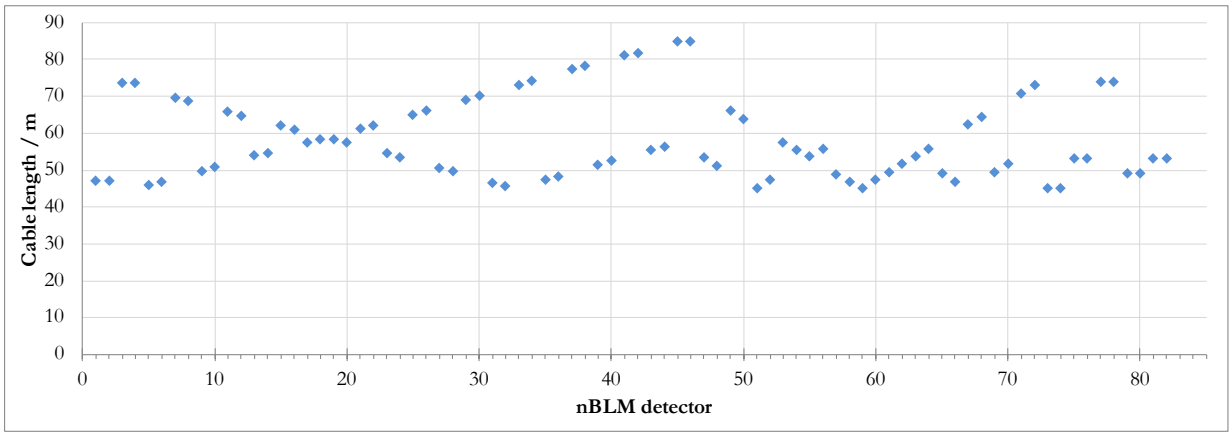

Figure 9: Estimated nBLM signal cable lengths.

Rack	Det. count	Det. location	HV card count	HV card tag	Det. per HV card	Spare cables per rack
FEB-050ROW	74	MEBT–MB	1	HV1	24M+24D	2M+2D
			1	HV2	22M+22D	
			1	HV3	14M+14D	
			1	HV4	12M+12D+2M+2D	
SPK-010ROW	0	/	0	/	0	2M+2D
SPK-030ROW	0	/	0	/	0	2M+2D
SPK-050ROW	0	/	0	/	0	2M+2D
MBL-050ROW	0	/	0	/	0	4M+4D
HBL-090ROW	0	/	0	/	0	4M+4D
HEBT-030ROW	8	>MB	1	HV5	2M+2D+2M+2D +4M+4D	1M+1D
A2T-010ROW	0		0		0	1

Table 4: Summary of the nBLM system HV connections. The column marked as “Det. per HV card” indicates the number of detectors powered by each HV card. Note that each a detector needs two HV connections, one for mesh (M) and one for drift (D). The colours mark different detector groups as discussed in the text and shown on figure 10.

Rack	Det. count	Det. location	LV card count	LV card tag	Det. per LV card	Spare cables per rack
FEB-050ROW	74	MEBT–MB	1	LV1	6+6+6+6	2
			1	LV2	6+6+6+4	
			1	LV3	6+4+4	
			1	LV4	6+6+2	
SPK-010ROW	0	/	0	/	0	2
SPK-030ROW	0	/	0	/	0	2
SPK-050ROW	0	/	0	/	0	2
MBL-050ROW	0	/	0	/	0	4
HBL-090ROW	0	/	0	/	0	4
HEBT-030ROW	8	>MB	1	HV5	2+2+4	1
A2T-010ROW	0		0		0	1

Table 5: Summary of the nBLM LV connections. The column marked with “Det. per LV card” indicates the number of detectors connected to each LV card. The "+” sign is used to differentiate between the channels on a certain LV card. The colours mark different detector groups as discussed in the text and shown on figure 10

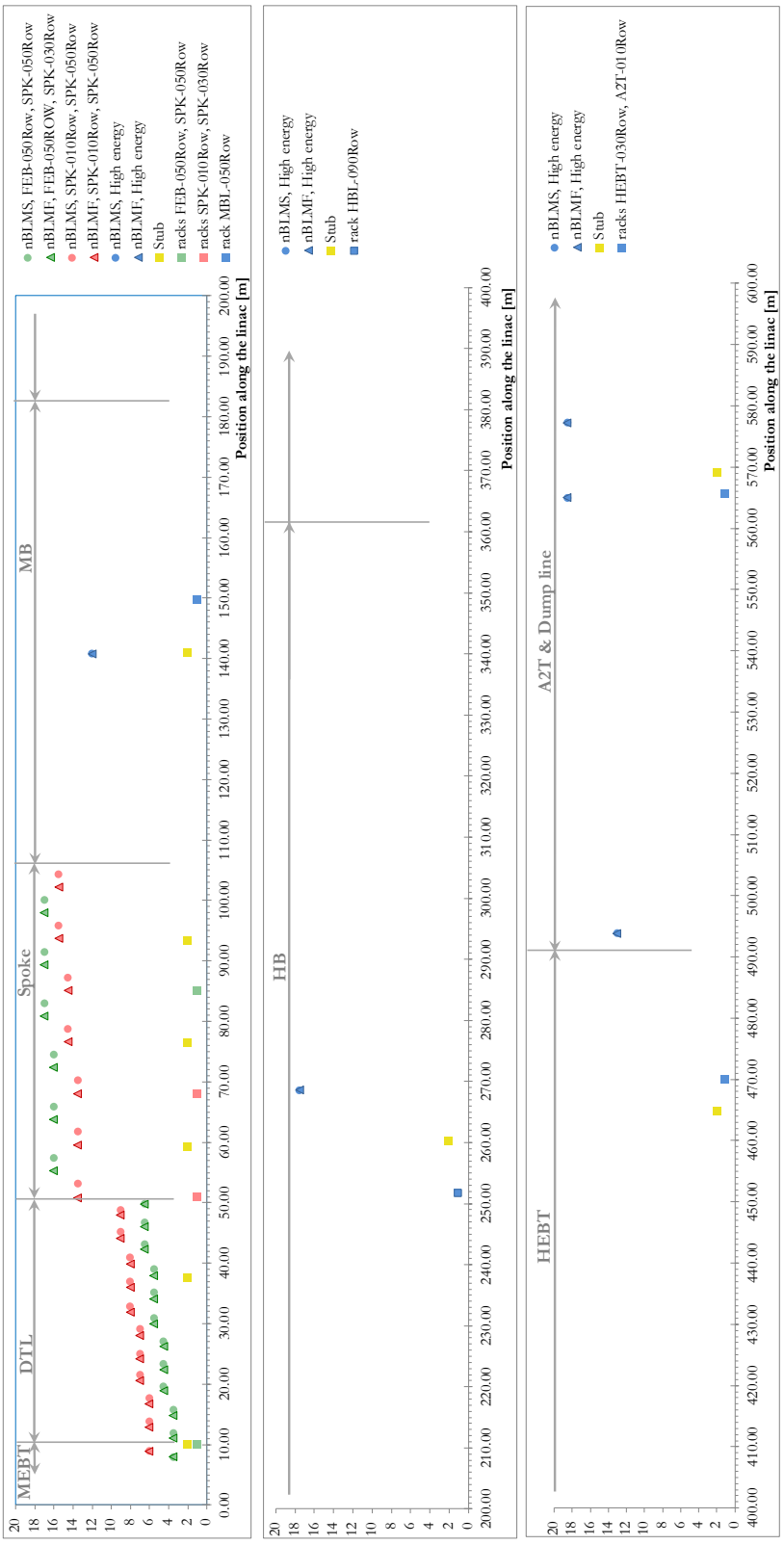

Figure 10: nBLM system signal cable layout, with horizontal axis running along the linac. See text for explanation.

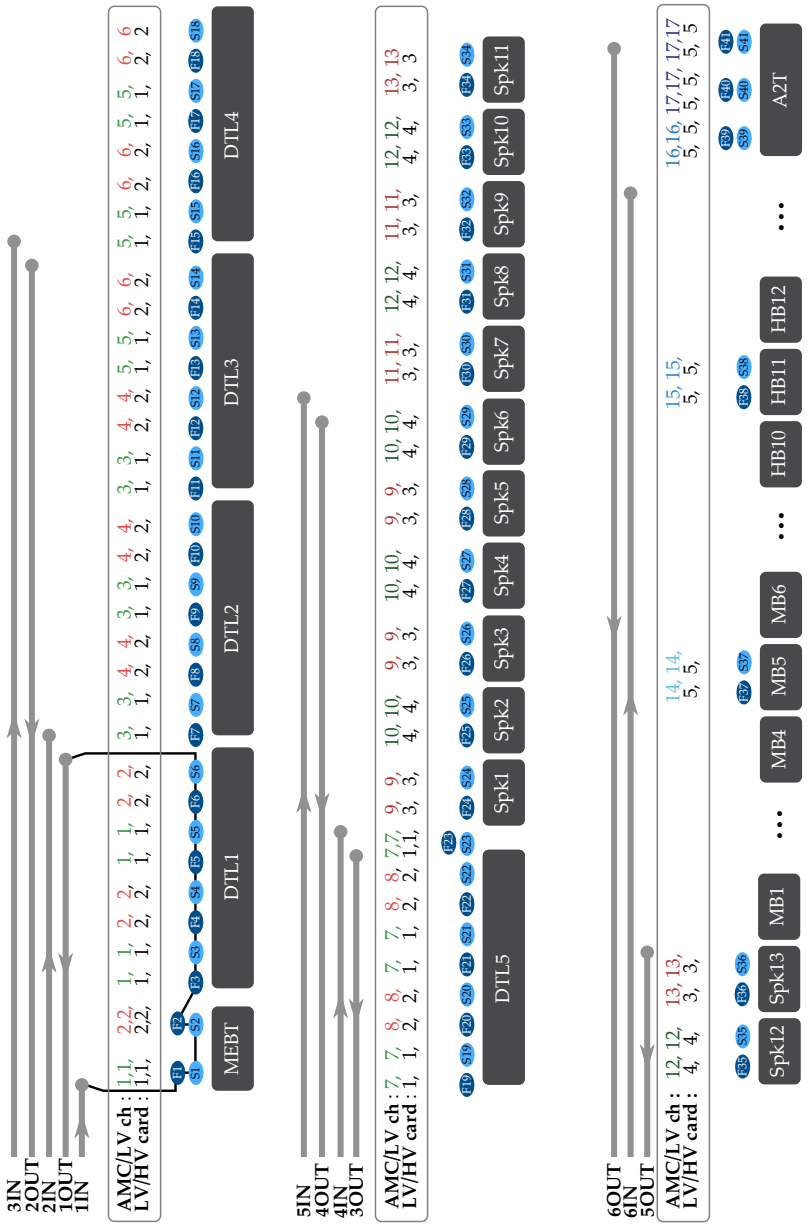

Figure 11: nBLM electronics and gas system layout along the linac.

5 Gas system

The nBLM system is based on gaseous detectors which need a continuous flow to insure a stable operation on a time scale of years. Thus, the system is designed to work in a re-circulation mode. A short summary of the nBLM gas system is given here, more details can be found in the document [13] focused on the gas system specifications.

Gas mixture used consist of He and 10 %CO_2. One IN and one OUT gas line is routed (together with 1 IN and 1 OUT spare line) through the FEB-100 building from the bottles in the storage area to the rack FEB-050Row:CNPW-U-001 located in FEB-090 building. The rack houses all the hardware for the gas control and monitoring. Here the IN/OUT line is split into 6 IN/OUT long haul lines which are passed through the FEB-090 shielding and tunnel wall to the accelerator tunnel. The lines end at different points along the linac where they are continued with polyurethane short lines. Thus, each pair of IN and OUT lines circulates gas through a group of 10–20 neighbouring detectors connected through short gas lines in series.

Approximate positions of the IN/OUT end points for the long pipes are indicated on figure 11. Additionally, full loop including the short line part is illustrated for one gas line (gas line1). Note that long and short lines are marked with grey and black colour respectively. Details about the number of neighbouring detectors on each long gas line are given in reference [36].

The detectors are flushed with 1-2L/h (IN/OUT lines) gas flow during the operation. However flushing is needed for a period of time before the operation as well in order to clean the tubes and detectors from possible dust particles and have pure gas which is not mixed with air. As a general rule of thumb the gas in the detectors needs to be changed 20 times before the detectors can be operated. Thus any intervention that requires opening the gas lines should be followed with a period of detector flushing. The requirement on pre-operational flushing time is lowered from 20 to 4 times, in case of shutdowns where the gas lines were kept sealed.

Table 6 summarises the estimations on time needed to flush the detectors for 1, 4 or 20 times with flow of 8L/h appropriate for pre-operational flushing. From the table it follows that $\sim$20h are needed to flush all detectors 4-times after intervention where the tubes stay sealed. In case of interventions where air enters the gas system the time increase to $\sim$100h, if all detectors and tubes need to be cleaned.

Detector location	Detector count	Pipe length [m]	Time to change gas 4 time [h]	Time to change gas 20 time [h]
MEBT-DTL1	36	12	4.02	20.12
DTL2+ DTL3	69	16	5.10	25.49
DTL4 + DTL5	101	16	5.55	27.75
SPK1-6	160	12	5.78	28.89
SPK7-13	204	14	6.70	33.52
MB-HB + A2T	1210	10	20.32	101.59

Table 6: Estimated times needed to flush the detectors one or several times [14, 36].

Details about the nBLM gas system design including information on control and monitoring are given in references [13, 39, 40].

6 Data processing

The focus of this chapter is the functionality of the FPGA based data processing. After listing the requirements related to the topic of data processing and monitoring, specifications of the data processing functionality are explained through a block diagram.

6.1 Requirements

The following gives a summary of both processing and monitoring requirements for the nBLM system:

1. The nBLM system shall be able to run standalone and can function even when the ESS linac is not in operation.

2. Each nBLM processing card shall be able to process and provide monitoring data for up to 8 input channels (8 nBLM detectors) simultaneously.

3. The signal from each channel shall be digitised and sampled at minimum 250MS/s.

4. All BLM systems shall follow the same approach where applicable (same monitoring data, user panels, ...).

5. Monitoring data shall be available to the user in the control room either:

   (a) **On demand** through the Data-On-Demand functionality. Details of the DoD concept is available in [29],

   (b) or **periodically** with the highest frequency equal to the nominal machine repetition rate of 14 Hz.

6. Requirements on data available to the user on demand (DoD data):

   (a) This data shall be continuously buffered and accessible to the user without stopping the data processing or buffering.

   (b) Minimum 3 consecutive pulse periods of raw data and 100 pulse periods of processed data shall be available to the user for retrieval on demand. Here the pulse period is defined as 1/(14 Hz).

   (c) The user shall be able to set pre– and post–trigger. Note that here the trigger tags a particular pulse period.

   (d) In case of raw data, the post and pre–trigger can be at minimum set to select from 2 pulse periods before to 2 pulse periods after the tagged pulse period (in addition to the tagged pulse), giving together minimum 3 consecutive pulse periods per request.

(e) In case of processed data, the post and pre–trigger can be at minimum set to select from 99 pulse periods before to 99 pulse periods after the tagged pulse period (in addition to the tagged pulse), giving together minimum 100 consecutive pulse periods per request.

7. There shall be at minimum three different types of trigger requests that can issue a retrieval of the buffered DoD data:

   (a) **Post–mortem**: on post–mortem event when one of the systems connected to the machine protection system drops the BEAM_PERMIT signal.

   (b) **Periodic**: for example once per day we want check the full history of neutron counts over several pulses.

   (c) **Conditional**: when certain conditions are reached in one of the systems with available DoD functionality (for example in nBLM, when monitored pedestal value reaches a certain limit).

   The user is responsible to configure each of these DoD trigger requests. This includes enabling channels, per– and post–trigger, periodicity in case of 7b and conditions in 7c).

6.1.1 Relaxed minimum requirements on nBLM DoD data

The requirement of buffering raw data continuously poses a challenge to the nBLM data processing with selected digital platform. Therefore the above stated requirements on the nBLM DoD data have been temporarily relaxed. In the relaxed form of the requirements the user shall be at minimum able to extract the following on each DoD trigger request:

- Limited amount of raw data as described below and
- minimum 100 pulse periods of neutron counts buffer (marked as CB2 on 12, see section 7.1 for definition) for minimum 6 channels.

The pulse period is again defined as 1/(14 Hz). It is acceptable to provide the same functionality over multiple AMC cards.
Regarding the limited amount or raw data available to the user on demand, either of the two options below is acceptable as the minimum:

1. Minimum 2 channels with continuous sampling. Requirements on full time window of extracted data:
   - Minimum 3 consecutive pulse periods of raw data shall be available to the user.
   - The user shall be able to set pre– and post–trigger. Note that here the trigger tags a particular pulse period.

- The post and pre–trigger can be at minimum set to select from 2 pulse periods before to 2 pulse periods after the tagged pulse period (in addition to the tagged pulse), giving together minimum 3 consecutive pulse periods per request.

2. Minimum 6 channels sampled only in a time window inside each pulse. This time window is referred to as the "unit sampling time window", while the "full sampling time window" represents the time window covering several consecutive unit time windows extracted on a DoD trigger. Requirements on the unit and full sampling time window:

   - Size and position of the unit sampling time window inside the pulse are configurable for each channel separately. All unit sampling time windows have the same settings for a given DoD request. The unit sampling time window position can be counted relative to the BEAM ON or RF ON period.
   - Minimum size of the unit sampling time window shall be 9 ms (i.e. 3 ms$\pm$3 ms to be able to capture the BEAM ON period inside the pulse).
   - Full sampling time window size: at minimum 3 sampling time windows of data is available to the user on demand.
   - The user shall be able to set pre- and post–trigger of the full sampling time window size. The post and pre-trigger can be at minimum set to select from 2 unit sampling windows before to 2 unit sampling windows after the tagged pulse period (i.e. tagged unit sampling time window), giving together minimum 3 consecutive unit sampling time windows of raw data per DoD request.

6.2 Specifications on data processing

A block diagram representing an overview of the FPGA functionality for one nBLM channel (detector) is shown on figure 12. A brief summary is given in this section. In addition to this, neutron detection algorithm, per–processing and buffering of data on demand are illustrated in the reference code given in reference [34].

6.2.1 “Raw data type selector” block

This block switches between two options for the input raw data:

- Real raw signals produced by a detector channel, to be used during normal linac operation.
- Simulated data or previously measured data provided by the user in a form of a data file. This option is used when system performance validation is needed.

The user is able to select between the two options on the fly.

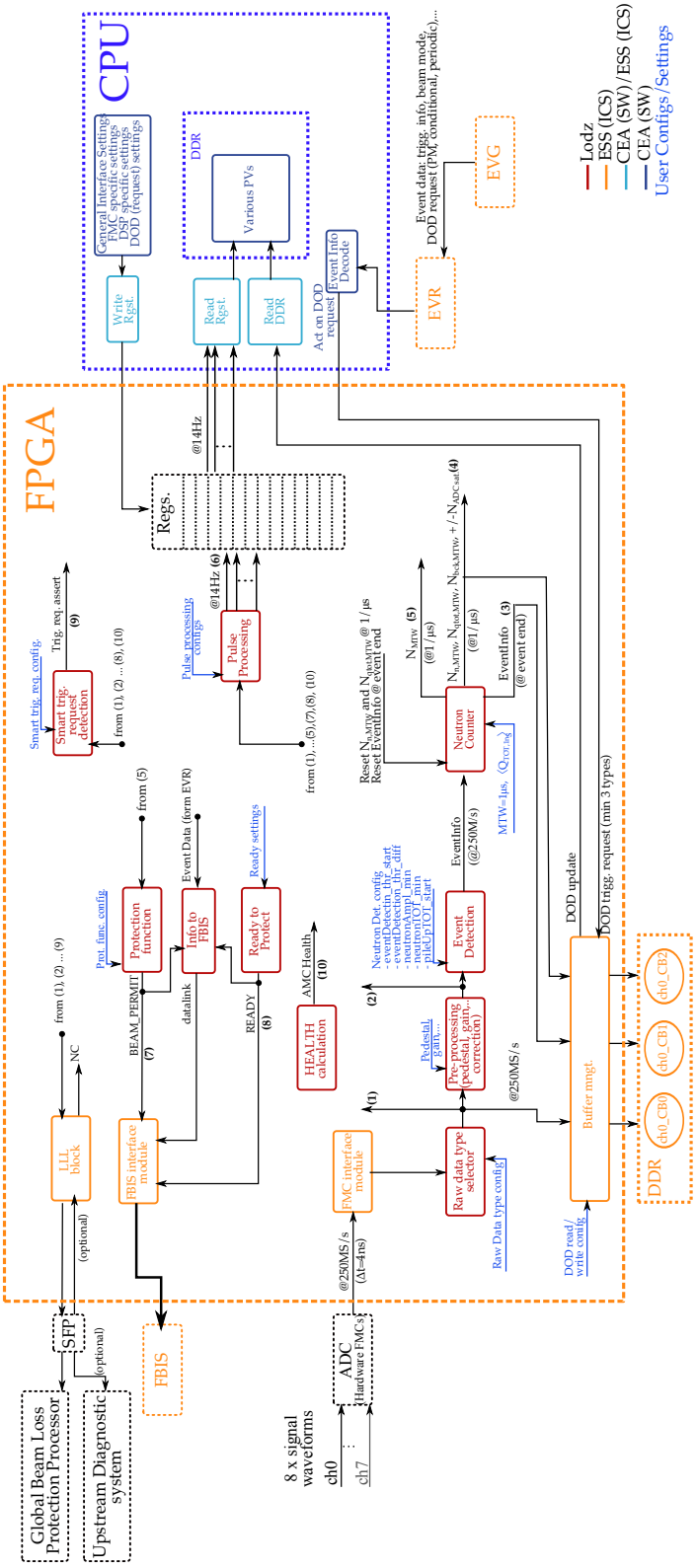

Figure 12: Block diagram of data processing in the nBLM system [33].

6.2.2 "Pre–processing" block

The input signal is sampled by the ADC FMC with a 250MS/s sampling rate. This raw data is first pre–processed, which currently includes only pedestal subtraction. Pedestal value is a setting for each channel separately and is provided by the user.

Potential upgrades of this block include corrections for cable distortion and FEE gain degradation due to the radiation induced damage.

6.2.3 Neutron detection algorithm

The description of neutron detection algorithm given in this section in general follows [30] with the exception of event detection threshold definition. Equal rising and falling edge values are considered in the referenced document, while here they are considered different in value. Additionally, the discussion here takes into account that the real nBLM signals are negative, while positive signals were assumed in the referenced document for simplicity.

The same neutron detection algorithm is used for both slow and fast nBLM detectors, the only difference is in algorithm settings set by the user, namely:

- `eventDetThr_start`, – falling (start) edge event detection threshold.
- `eventDetThr_diff` – difference between falling and rising edge event detection threshold, namely

$$\texttt{eventDetThr\_diff} = \texttt{eventDetThr\_end} - \texttt{eventDetThr\_start}, \qquad (1)$$

  where `eventDetThr_end` represents rising (end) edge event detection threshold. For a well functioning algorithm $\texttt{eventDetThr\_diff} > 0$.
- `neutronTOT_min` – minimum signal length (i.e. time-over-threshold or TOT) to identify a neutron.
- `pileUpTOT_start` – minimum signal length to identify pile-up and maximum to identify single neutron.
- `neutronAmpl_min` – maximum amplitude to identify neutron(s).
- $\left\langle \texttt{Q\_TOT}_{1n} \right\rangle$ – average charge for single neutron event.

The basic idea behind the neutron detection is to identify and distinguish between 3 types of interesting events: **single neutron**, **neutron pile-up** and **non-neutron events**. Then one of the two methods for neutron counting is used to estimate the neutron count every time a neutron event (single neutron or pile-up) is detected:

1. **Single neutron counting method** is in general used when a single neutron is identified. It is based on simply increasing the counter by 1.

2. **Charge method** is in general used for pile-up events. It is based on summing the charge contained in such an event and compare it to the average value for the charge found in events identified as single neutrons.

Note however that certain exceptions hold to the general rule mentioned above (see section 6.2.3.3).

6.2.3.1 Event types

The j-th event is identified as a **single neutron** when all the following conditions are satisfied:

- Event Time-Over-Threshold ($\texttt{TOT}_j$) is within a certain range, namely if

$$\texttt{neutronTOT\_min} \leq \texttt{TOT}_j < \texttt{pileUpTOT\_start}. \tag{2}$$

- Event amplitude is below a certain limit, specifically if

$$\texttt{peakValue}_j \leq \texttt{neutronAmpl\_min}. \tag{3}$$

Similarly, the j-th event is identified as **neutron pile-up** when both conditions stated below are met:

- Event TOT is above the upper limit for single neutron, that is if

$$\texttt{TOT}_j \geq \texttt{pileUpTOT\_start} \tag{4}$$

- Event amplitude is below the same limit as for a single neutron, which translates to the same condition as given in equation 3.

Non-neutron events can further be classified into **background** and **false events**. The former is due to γ photons and potentially other background particles, while the latter is caused by noise and potentially sparks.

It would be an advantage if the system could provide some estimation on the γ background which can be approximated with background events. In theory single γ events are expected to be shorter than single neutrons if constant threshold for TOT estimation is used. This makes identification of background events difficult without introducing additional settings and complexity. Since the main goal of nBLM system is to provide neutron counts, a simple approach has been adopted, where the background events are approximated as events which qualify as neutrons in terms of TOT but not amplitude. Namely, a background event satisfies the following condition:

$$\begin{aligned} \texttt{TOT}_j \geq \texttt{neutronTOT\_min}, \quad \text{and} \\ \texttt{peakValue}_j > \texttt{neutronAmpl\_min}. \end{aligned} \tag{5}$$

However this definition can include baseline fluctuations, though these are expected to be minimal if detector is performing well and the algorithm is configured correctly.

6.2.3.2 Definition of `EventInfo`

The task of neutron detection algorithm is to provide:

- Two numbers representing neutron counts calculated by each of the two methods reported at the end of every Monitoring Time Window (MTW), currently set to 1 µs.
- Information about each detected event, combined here in a structure of various event related variables defined as `EventInfo`.

In particular, `EventInfo` contains the following information about the j-th event (see figure 13.

- $\texttt{TOT}_j$ – time over threshold, represents the number of samples below or equal to the threshold for event detection.
- $\texttt{Q\_TOT}_j$ – charge integrated over the $\texttt{TOT}_j$ time window.
- $\texttt{peakValue}_j$ – amplitude, i.e. minimum signal found inside the $\texttt{TOT}_j$ time window.
- $\texttt{TOTstartTime}_j$ - time bin index of the event start (here measured from the start of MTW where the event has started).
- $\texttt{peakTime}_j$ - time bin index at the $\texttt{peakValue}_j$ (measured from $\texttt{TOTstartTime}_j$).
- $\texttt{TOTvalid}_j$ – true if condition $\texttt{TOT}_j \geq \texttt{neutronTOT\_min}$ is met, otherwise false.
- $\texttt{peakValid}_j$ – true if condition $\texttt{peakValue}_j \leq \texttt{neutronAmpl\_min}$ is met, otherwise false.
- $\texttt{pileUp}_j$ – true when pile up condition is reached, namely $\texttt{TOT}_j \geq \texttt{pileUpTOT\_start}$ and $\texttt{peakValid}_j = \texttt{true}$.
- $\texttt{MTWindx}_j$ – index of the MTW where the event started (or a time stamp defining the MTW start).
- $\texttt{isTruncated}_j$ – true when event ends at the edge of a MTW.
- $\texttt{isPart2}_j$ – true when event is a continuation of the previous event which ended on the edge of MTW.

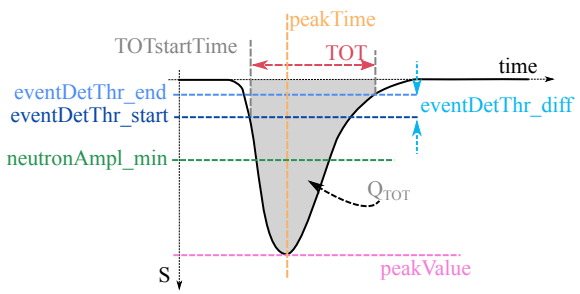

Figure 13: Definition of `EventInfo` structure elements and neutron algorithm settings.

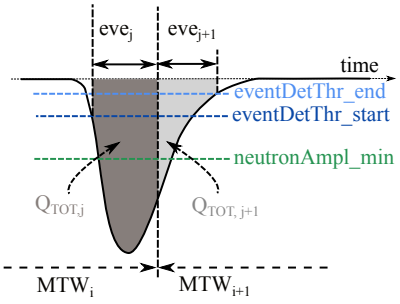

Figure 14: Example of a neutron signal extending over the edge of MTW, which satisfies the condition in item 2b (section 6.2.3.3) to be split in two events.

6.2.3.3 Definition of "Interesting event"

The algorithm must provide the information without unnecessary delays. This is achieved by requiring several exceptions to the basic rule of when each of the counting methods stated at the beginning if section 6.2.3 is used. These exceptions are related to handling the events that extend over the edge of a MTW (see figure 14). They lead to necessity of splitting the events at MTW edges in certain cases which results in the following definition of an **interesting event**:

1. An interesting event j starts either:

   (a) when the signal falls below a certain threshold – falling edge event detection threshold, i.e. when

   $$s(t_k) \leq \texttt{eventDetThr\_start}, \quad \text{and} \tag{6}$$
   $$s(t_{k-1}) > \texttt{eventDetThr\_start}, \tag{7}$$

   where $s(t_k)$ stands for signal at time t_k marking the start of the event, or

   (b) if the previous event ended on a MTW edge and the current event is a continuation with signal below rising edge event detection threshold, i.e. if

   $$\texttt{isTruncated}_{j-1} = \texttt{true} \quad \text{and} \tag{8}$$
   $$\texttt{TOTstartTime}_j = 0 \quad \text{and} \tag{9}$$
   $$s(t_{k-1}) > \texttt{eventDetThr\_end}. \tag{10}$$

   where $s(t_k)$ again marks start of the event. In this case $\texttt{isPart2}_j$ is set to $true$, otherwise it stays at its default value `false`. Note that this conditions is needed due to the hysteresis in the event detection threshold which leads to different falling and rising edge thresholds for event identification. The condition ensures that the second part of a signal that was split on a MTW edge is not ignored in case its signal lies within the rising and falling edge event detection thresholds.

2. An interesting event ends either:

   (a) one time bin before the signal increases above the rising edge event detection threshold, i.e. at time t_{k-1} if signal $s(t_k) > \texttt{eventDetThr\_end}$, or

   (b) on MTW edge, if it is reached before the condition in item 2a is met and conditions for single neutron or pile-up have already been met, or

   (c) on MTW edge, if condition in 2a has not been met and the $\texttt{TOT}_j$ is above a certain limit, currently set to

   $$\texttt{TOT}_j \geq \texttt{TOTpileUp\_start}. \tag{11}$$

   In the last two cases $\texttt{isTruncated}_j$ is set to `true`, otherwise it stays at its default value `false`.
   The last condition is necessary to avoid cases where a non-neutron event extends over several MTWs with no information on count available over this period.

6.2.3.4 Neutron counts

The number of neutrons at the end of each MTW is calculated as

$$N_{MTW,i} = N_{n;MTW,i} + N_{qtot;MTW,i} = \sum_{j=1}^{n_{eve;MTW,i}} (N_{n,j} + N_{qtot,j}). \tag{12}$$

where index j runs over the events inside the i-th MTW, while $N_{n;MTW,i}$ and $N_{qtot;MTW,i}$ represent the neutron counts inside the i-th MTW estimated through single neutron counting method and through charge method respectively. Both are a sum of contributions from each neutron event found inside this MTW.

With all this in mind the following rule holds regarding the usage of the two counting methods:

1. **Single neutron counting method**
   This method is used whenever a single neutron event has been identified, namely when the following holds at the end of j-th event:

   $$\texttt{TOTvalid}_j = \texttt{true} \quad \text{and} \tag{13}$$
   $$\texttt{peakValid}_j = \texttt{true} \quad \text{and} \tag{14}$$
   $$\texttt{TOT}_j < \texttt{TOTpileUp\_start}. \tag{15}$$

   When the above condition is met $N_{n,j}$ is set to 1 and $N_{qtot,j}$ remains 0.

2. **Charge method**
   Charge method is used in the following cases of events:

   (a) If j-the event has been identified as a pile-up event, that is when $\texttt{pileUp}_j = \texttt{true}$ at the end of the event.

(b) If an event ended on a MTW edge and has been identified as a single neutron or pile-up event, i.e. if at the end of j-th event

$$\texttt{TOTvalid}_j = \texttt{true} \quad \text{and} \tag{16}$$
$$\texttt{peakValid}_j = \texttt{true} \quad \text{and} \tag{17}$$
$$\texttt{isTruncated}_j = \texttt{true}. \tag{18}$$
$$\tag{19}$$

(c) If the previous event ended on the previous MTW edge and was identified as a single neutron or pile-up, while the current event is its a continuation; i.e. when at the end of j-the event

$$\texttt{TOTvalid}_{j-1} = \texttt{true} \quad \text{and} \tag{20}$$
$$\texttt{peakValid}_{j-1} = \texttt{true} \quad \text{and} \tag{21}$$
$$\texttt{isTruncated}_{j-1} = \texttt{true} \quad \text{and} \tag{22}$$
$$\texttt{isPart2}_j = \texttt{true}. \tag{23}$$

The last two cases correspond to a signal that was split in two events at the MTW edge (see figure 14).
For j-th event satisfying one of the conditions above, the neutron counts are set as

$$N_{n,j} = 0 \tag{24}$$
$$N_{qtot,j} = \frac{\texttt{Q\_TOT}_j}{\left\langle \texttt{Q\_TOT}_{1n} \right\rangle}, \tag{25}$$

where $\left\langle \texttt{Q\_TOT}_{1n} \right\rangle$ represents the average value of the charge $\texttt{Q\_TOT}_j$ for single neutron events. Note that this is a user setting. Its value is also being periodically monitored (see table 7) and a warning or alarm is raised if the two values (i.e. set and monitor value) differ over acceptable limits.

6.2.3.5 Blocks related to neutron detection

The neutron detection algorithm is performed through "Event Detection" and "Neutron Counter" blocks in the block diagram. The role of these two blocks can be summarised as:

- "Event Detection" block detects start of an interesting event and updates the `EventInfo` structure with a frequency of the raw data sampling rate of 250 MHz.
- "Neutron Counter" block has two functions:
  - It keeps track of neutron counts per MTW calculated with the two methods ($N_{n,MTW}$ and $N_{qtot,MTW}$) and resets them at the end of each MTW.
  - Additionally, if previously mentioned conditions for ending an event are met, the "Neutron Counter" block ends an event and resets the `EventInfo`.

6.2.4 "Protection Function" block

The "Protection Function" block takes neutron counts N_{MTW}, arriving at 1MHz rate (see eq. 12) as the input. The primary task of this blocks is to assess whether conditions to inhibit beam production have been met. In case they have, the block drops the BEAM_PERMIT signal on the line connected to the FBIS through the FBIS interface. FBIS then further handles stopping of the beam production. Note that, though binary from perspective of information, the BEAM_PERMIT signal is continuously transmitted to FBIS (not in frames).

Each AMC provides one aggregated BEAM_PERMIT signal independent of the number of detector channels connected to it. The BEAM_PERMIT calculation starts with calculating the value for each channel separately, BEAM_PERMIT_c (c runs over all channels on the AMC). This is performed by checking if the beam inhibit condition on each particular channel has been reached. The final BEAM_PERMIT is then determined by AND–ing the BEAM_PERMIT_c of all channels that are not masked out from the calculation:

$$\text{BEAM\_PERMIT} = \bigvee_{c \notin \text{masked}} \{\text{BEAM\_PERMIT}_c\}. \tag{26}$$

Note that some detectors might be too noisy and may thus be excluded from the final BEAM_PERMIT calculation. In addition to this, there might be situations when it is desirable to exclude certain detectors from the calculation (controlled losses, detectors close to Faraday Cup when it is inserted). For this reason, each channel can be masked out from the BEAM_PERMIT calculation.

In order to avoid spurious BEAM_PERMIT drops based on assessment of a single data point

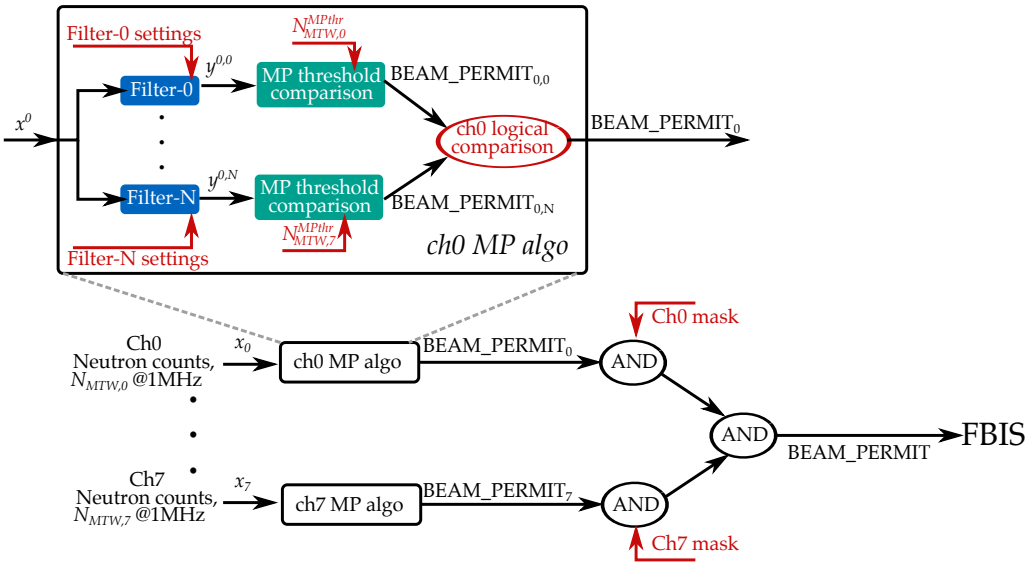

Figure 15: Schematic of the BEAM_PERMIT calculation for each AMC. Red colour marks configurables.

on a single channel polluted with noise spike(s), some filtering of the input neutron counts is planned. Three different types of filtering algorithms have been identified so far as interesting for this purpose: relaxation filter, X/Y algorithm, moving average filter or simple average. Each filter instance is applied to neutron counts per MTW for each channel. For a given channel c the output of a filter is recalculated on each new neutron count data point and compared to a certain machine protection threshold value ($N^{\mathrm{MPthr}}_{MTW,c}$). If the output of the f-th filter on c-th channel is above this value, then the beam inhibit condition has been reached and the corresponding BEAM_PERMIT$_{c,f}$ for the filter and channel in question is dropped to down state (0), otherwise it is left at up state (1). One or several selected filters are considered in the channel BEAM_PERMIT$_c$ calculation by logically combining their BEAM_PERMIT$_{c,f}$ through AND or OR logical operators. Selection of the filters and the sequence of logical operators used in the beam permit calculation can differ from channel to channel and is configurable by the user. A schematic representation of the BEAM_PERMIT calculation for each AMC is summarised on figure 15.

In the following a short description of filtering algorithms of interest is given.

1. **Moving average**
   Denoising in case of moving average is based on calculating a local average over the time window of t_{MA} containing the last n input data points:

$$y_k = \frac{1}{n}\sum_{l=0}^{n-1} x_{k-l}. \tag{27}$$

   Here x_k and y_k represent filter input and output values respectively. With increasing the number of points included in the average, n, smoothing is improved, though on the expense of increasing the delay of the output y compared to the input x.

2. **Relaxation filter**
   Relaxation filter is an IIR (Infinite Impulse Response) filter of the first order with a feedback. It takes a weighted sum of the old output y_k and the new input value x_k as the new output y_{k+1}:

$$y_k = \frac{m-1}{m} y_{k-1} + \frac{1}{m} x_k \quad \text{or} \tag{28}$$

$$y_k = \lambda y_{k-1} + (1-\lambda) x_k, \quad \text{with} \quad \lambda = \frac{m-1}{m}. \tag{29}$$

   The parameter λ can take values $0 < \lambda < 1$. If $m \to \infty$ then $\lambda \to 1$ and the filter forgets the past values to a smaller extent. With λ very close to 1 the smoothing power is comparable to the case of a moving averag filter with a large number of points.
   The continuous equation governing the relaxation filter can be written as

$$\tau \frac{dy}{dt} = -y + x. \tag{30}$$

where $\lambda = 1 - dt/\tau$. The equation is equivalent to a 1-st order low–pass filter with time constant τ. The difference between relaxation filter and a typical low–pass filter is in the cutoff frequency. In case of a low–pass filter the signal of interest is in the passband and the cutoff frequency is set above the highest acceptable frequency. On the other hand, the interesting signal is in stopband in case of a relaxation filter and the cutoff frequency is set below the lowest acceptable frequency.

3. **X/Y algorithm** For a given channel c, the algorithm takes Y last number of counts on this channel as an input, x_k. Each of these data points is compared to the machine protection threshold ($N^{\mathrm{MPthr}}_{MTW,c}$). If X out of Y last data points exceed the threshold, then the BEAM_PERMIT$_{c,X/Y}$ attributed to this filter and channel c is dropped, otherwise it stays in up state. Note that in this case the filter output is already the beam permit state itself and not the smoothed neutron counts as in the case of the two filters mentioned above.

4. **Simple average**
   Here the average value is calculated over a certain time window inside the pulse period. The calculation is caried out with a fresh set of values on each calculation restart. The values are thus not carried forward across restarts.

Five filter instances are anticipated to be tested during the beam commissioning of the nBLM when protection algorithms are planned to be verified, namely relaxation filter, X/Y algorithm, 2 different moving average filters differing in time constants (fast with $t_{MA,1} \sim 1\,\mu s$, medium with $t_{MA,2} \sim 100\,\mu s$) and a simple average over beam pulse (over the BEAM_ON period). However the protection functions are planned to be co-developed across the beam instrumentation systems providing beam loss information. Hence further developments are foreseen following experience gained through system commissioning and ongoing simulations.

Another way to limit the spurious BEAM_PERMIT drops, is to base the BEAM_PERMIT calculation on requiring coincidences between neighbouring channels inside certain time windows. This option requires a functioning LLL block and is foreseen for the upgrade of the system.

6.2.5 Signals propagated to FBIS

In addition to the BEAM_PERMIT, the following signals are provided to FBIS by each AMC card:

- READY signal.
  This signal is dropped whenever the system is not ready to protect the machine. Currently the only potential usage for this signal is during the start up periods when system is collecting enough statistics for the user to check and/or set proper settings for the system (for example, pedestal or $\langle \mathrm{Q\_TOT}_{1n} \rangle$). Like BEAM_PERMIT this signal is continuously transmitted to FBIS through "Ready to Protect" block.

- Datalink.
  The Datalink signal is transmitted with certain frequency and may contain the following information
  - Redundant (current) BEAM_PERMIT signal.
  - Redundant (current) READY signal.
  - Current Beam Mode and Beam Destination configured into the processing card (or as received from EVG).
  - Health status of the link, which is used by the FBIS to diagnose the problems in connection between the FBIS and the processing card. The health status is simply a value of the counter incremented in every packet/frame sent to FBIS.
  - AMC health status indicating the status of the data processing running on the AMC in question (see 6.2.10).

The exact definition of these signals is not fully finalised and is under discussion with the machine protection team. First draft of the interface document between BLM systems and FBIS is available in reference [44].

6.2.6 "Pulse Processing" block

The role of this block is to provide first stage of data post–processing. It transforms its inputs into variables with the fastest outgoing frequency of machine repetition rate (14 Hz) which can further be handled by the EPICS based monitoring and controlling software. The result of this second stage post–processing, is a set of periodically updated data available to the user in the control room for monitoring. Full list of nBLM variables that are monitored periodically (periodic data) is available in table 7.

6.2.7 Buffering of data on demand

Certain processed data as well as raw signals are being buffered and available to the user on demand through the Data-On-Demand (DoD) functionality [29]. The data retrieval can start when the DoD buffer receives the DoD trigger request distributed by the master (EVG). In general the request can be issued either (see requirement 7) in subsection 6.1):

- Through the "Smart Trigger" by a certain system (nBLM, icBLM, BCM, etc, conditional trigger).
- On each post–mortem event.
- Periodically (periodic trigger).

List of nBLM data that can be retrieved through the DoD functionality is given in subsection 7.1.

6.2.8 "Smart Trigger" block

As stated in requirements in section 6.1, the DoD data can be retrieved by issuing a DoD trigger request, where minimum 3 different types of triggers are foreseen: post–mortem, periodic or conditional. Note that not all will be enabled at all times, the user enables and configures one or more of them when needed.

The "Smart Trigger" block is responsible for issuing a conditional DoD trigger. It takes various inputs, which can be considered as waveforms (for example, neutron counts sampled at 1 MHz), and asserts a trigger request (conditional trigger) on the output in case certain conditions have been met. The conditions are configurable and set by the user. The trigger assert is then propagated to the master (EVG) which can distribute this trigger request to all systems configured to listen to it. Although "Smart Trigger" has been conceived as part of the DoD concept, it can in principle provide triggers to anything that is listening.

The definition of "Smart Trigger" functionality is a part of the DoD concept and should be consistent among all systems partaking in the DoD service. As the DoD feature has not been developed far enough to include this definition, an initial version has been developed for the case of nBLM and icBLM systems. Though further changes and augmentations are expected in the near future as the DoD concept matures.

In the initial version of "'Smart Trigger" definition, the conditional trigger is asserted whenever a condition expression unit is satisfied. One conditional expression unit is available per each detector channel and is defined as

$$\mathscr{C}(a_i(w_j), v(a_i)) = a_i(w_j) \overset{\text{compare}}{\Longleftrightarrow} v(a_i), \tag{31}$$

where w_j represents the j-th input waveform available to the "Smart Trigger" block, while $a_i(w_j)$ indicates current value for its i-th attribute. The later is compared to the value $v(a_i)$ with operator $\overset{\text{compare}}{\Longleftrightarrow}$ which can either be $>$, $<$, $\geq$, $\leq$ or $=$. Both operator type and value $v(a_i)$ are set by the user.

A general rule is that the user is able to configure a conditional trigger on any waveform w_j that can be visually inspected. In case of nBLM system the following input waveforms are available to the "Smart trigger" block as indicated in the block diagram:

- Raw data – marked with (1) in the block diagram.
- Pre–processed data – (2).
- Processed data:
  - Elements of EventInfo block – (3).
  - Neutron counts – (4) and (5).
- Outputs from the pulse processing block – (6).
- Protection function outputs – (7).

- READY status signal – (8).
- AMC health status – (10).

The numbers attributed to the items in the above list are consistent with the numbers indicated on figure 12. It may be too expensive to include smart triggering of all input waveforms on the firmware level. Thus smart triggering on certain waveforms (for example pulse processing block outputs) is moved to the software level in the actual implementation. For further details see [31, 37].

List of attributes that can be assigned to each input waveforme are common to all systems with available DoD functionality and are subjected to the DoD specifications. The list in the first version of the nBLM and icBLM "Smart trigger" definition includes:

- threshold on rising edge and
- threshold on falling edge.

6.2.9 "Low Latency Link" (LLL) block

This block is part of a concept foreseen for future upgrade and provides an option to combine the data coming from different system. An example of this would be, identification of coincident signals between two different BLM channels that are not processed by the same BEE card or even between a BLM channel and certain condition on a BCM channel.

6.2.10 "HEALTH Calculation" block

The goal of this block is to diagnose potential problems in data processing chain and report the "AMC health" status at a given ferquency. Calculation of the "AMC health" among other includes checking whether any part of the data procesing line is frozen or malfunctioning as well as status of the ADC FMCs. The exact calculation depends on the FW implementation details and is thus described in the document focused on the FW implementation description in reference [37].

7 Monitoring and control

Specifications related to control and monitoring of the HV, LV and gas system are given in [31], while the topic of processed data monitoring is covered here.

Requirements on monitoring of processed data have been specified in subsection 6.1, which collects all general requirements related to the nBLM data processing and monitoring. Hence, this section focuses solely on specifying the processed data to be monitored together with relevant settings available to the user.

Note that all waveforms will be reported according to the ESS diagnostic standards and will have standard attributes (settings) associated to them. As this is under development, some of the settings are given in this document as a starting point. Note also that all monitoring data will have a time stamp of their origin attributed to them.

7.1 Monitoring of processed data available on demand

Three different types of data are available on demand for each channel (detector):

1. **Raw data**.
   As stated in requirements in section 6.1, user in the control room is able to retrieve minimum 3 machine pulse periods of raw data for each channel on demand. This data stream is buffered in the buffer marked as CB0 on figure 12.

2. First stage of processed data – **EventInfo structure** (see section 6.2.3.2)
   The structure contains information about the reconstructed event. As stated in requirements, the user is able to retrieve minimum 100 pulses of data for each channel on demand. The buffer reserved for buffering this data is labeled as CB1 on figure 12. The data is written to the buffer every time an "interesting event" ends. The time between two successive interesting events (arrival time) is statistical in its nature, thus in this case the data is not buffered with a fixed rate. Note that since the interesting events include both neutron, background and noise events, the distribution of arrival time depends on various factors like neutron algorithm settings, electronics bandwidth, detector properties, FEE settings and environment.

3. Second stage of processed data – **Neutron counts**
   The buffer holding this data is marked as CB2 on figure 12. This data stream is buffered at a fixed rate of 1 MHz, where each sample contains the following information:

   (a) A pair of **neutron counts** at the end of each MTW (see section 6.2.3.4).
   MTW is currently set to 1 µs. The pair of counts consist of counts calculated by the two different methods (section 6.2.3.4). The user is able to retrieve minimum 100 pulse periods of this data (see requirements in section 6.1 for details).

(b) Number of positive and negative **ADC saturation** in raw data per each MTW. These numbers could potentially be used to diagnose bad operation conditions or sparks in the detector.

(c) **Charge in background events** at the end of each MTW (see equation 5 in section 6.2.3.1 for definition).

(d) **Total charge** per each MTW (integral over full MTW).

Some details and conservative initial estimations regarding the frequency and size of the data is available in [32].

The following summarises the information that can be extracted from the DoD data for each nBLM detector channel and available to the user:

1. **Raw data buffer – CB0**.

   (1) A waveform of raw unprocessed signal with configurable start time and length. The maximum time length is not shorter than 9 ms. The user can select to overlay several consecutive waveforms with 1/(14 Hz) distance (i.e. 1 waveform per pulse) in order to be able to compare time structures in consecutive pulses.

   (2) Statistics of displayed waveforms from (1). The statistics is calculated on a configurable time window inside the displayed waveform and includes average, variance, min and max value. Here the variance is defined as the average squared deviation from the average value, $\mathrm{Var}(x_i) = \sqrt{\langle (x_i - \langle x_i \rangle)^2 \rangle} = \sqrt{(\langle x_i^2 \rangle - \langle x_i \rangle^2)}$.

   (3) Same as item (1) but for pedestal corrected data. Here the pedestal value which is a setting for the pre-processing block (see section 6.2.2) is used for the calculation.

   (4) Same as item (2) but for pedestal subtracted waveforms in item (3).

2. **EventInfo buffer – CB1**.

   (1) 1D histogram of reconstructed event $\mathtt{peakValue}_j$. (event amplitude).

   (2) 1D histogram of reconstructed event $\mathtt{Q\_TOT}_j$.

   (3) 1D histogram of reconstructed event $\mathtt{TOT}_j$.

   (4) 1D histogram of reconstructed event $\mathtt{TOTstartTime}_j$.

   (5) 1D histogram of reconstructed event $\mathtt{peakTime}_j$.

   (6) 2D histogram of reconstructed event $\mathtt{peakValue}_j$ on y– and $\mathtt{TOT}_j$ on x–axis.

   (7) 2D histogram of reconstructed event $\mathtt{peakTime}_j$ on y– and $\mathtt{TOT}_j$ on x–axis.

   (8) 2D histogram of reconstructed event $\mathtt{Q\_TOT}_j$ on y– and $\mathtt{TOT}_j$ on x–axis.

   (9) 2D histogram of reconstructed event $\mathtt{peakValue}_j$ on y– and $\mathtt{peakTime}_j$ on x–axis.

   (10) 2D histogram of reconstructed event $\mathtt{Q\_TOT}_j$ on y– and $\mathtt{peakValue}_j$ on x–axis.

(11) 2D histogram of reconstructed event $\texttt{Q\_TOT}_j$ on y– and $\texttt{peakTime}_j$ on x–axis.

(12 — 16) Statistics associated with each 1D histogram above (items (1)–(5)): average, variance, min and max value of the sample together with the overflow and underflow information (number of hits under and above the histogram range respectively).

(17 – 22) Statistics associated with each 1D histogram above (items (1)–(5)): average, variance, min and max value of the sample together with the overflow and underflow information in all 8 direction of the histogram range (number of hits outside the range).

(23 – 27) Waveforms of $\texttt{Q\_TOT}_j$, $\texttt{TOT}_j$, $\texttt{TOTstartTime}_j$, $\texttt{peakTime}_j$ and $\texttt{peakValue}_j$ time evolution.

Histogram settings (number of bins, lower edge of the first bin, upper edge of the last bin) are configurable. In addition to this, the user can choose to combine the results with several past DoD dumps (with available EventInfo) into one histogram or overlay the histograms for each DoD dump.
The waveforms the definition as given in item (1) of item 1. with "raw unprocessed signal" replaced with appropriate quantity from the list above.
Note that since the neutron detection algorithm is designed to frame the events in MTWs, the real event attributes have to be reconstructed. An example analysis code for event reconstruction is available in reference [35]. The code was used for analysis of raw and processed data collected with IFC1410 base nBLM DAQ during the tests in Linac4 at CERN in December 2018.

3. **Neutron counts buffer – CB2**.

   (1) Waveform of neutron counts per MTW as calculated with single neutron counting method.

   (2) Waveform of neutron counts per MTW as calculated with charge method.

   (3) Waveform of total neutron counts per MTW (sum of the counts from both methods).

   (4) Waveform of total charge in neutron events per MTW. Note that this is calculated from item (3) with the use of average charge in single neutron event, $\left\langle \texttt{Q\_TOT}_{1n} \right\rangle$ (neutron det. algorithm setting, see section 6.2.3).

   (5) Waveform of charge in background events per MTW.

   (6) Waveform of total charge per MTW (integral over full MTW).

   (7) Waveform of number of positive ADC saturations per MTW.

   (8) Waveform of number of negative ADC saturations per MTW.

   (9) Statistics on all the above waveforms (items (1) – (8)).

   The waveforms and statistics follow the definition as given in items (1) and (2) of item 1. respectively with "raw unprocessed signal" replaced with appropriate quantity from the list above.

In addition to this, the information about the time stamp of the last DoD trigger request and its type (if available) is available to the user.

7.2 Monitoring of periodically available processed data

Monitoring data available to the user in the control room periodically is summarised in table 7. For definition of background and neutron events see section 6.2.3.1. For definition of EventInfo elements see section 6.2.3.2.

Note that losses scale with number of detected neutrons with scaling factor depending on the detector as well as its location, beam current and beam energy (i.e. loss scenarios). The identification of the loss source is not an easy task and in most of the cases not even possible without taking into account the information from several loss monitoring systems and channels. Thus, for each detector channel the losses are planned to be reported both as neutron counts and with a scaling factor calculated (and/or measured) by scaling to a selected loss scenario. For each detector the scenario is selected from a set of controlled loss scenarios that serve to verify the simulation (see section 8). The work related to this is ongoing.

Table 7: List of periodically available monitoring nBLM data with corresponding user settings labelled and indexed as S_{index}. Unless specified otherwise, the variable refers to one (detector) channel. Settings marked with $^{(*)}$ indicate that the same value is used for all channels. Data type can be a waveform (array) or scalar marked as w or s respectively. Column marked as "Source" specifies whether the calculation of the variable is expected to be performed on the firmware (fw) or the software (sw) level.

ID	Description	Type	Num. of el.	Update rate	Source	User settings	Comment
	Losses accumulated over certain period of time						
1	Loss over time T_1	s	1	$1/T_1$	sw	• $S^{(*)}_{1,...,7}$: times T_1,...T_7. • $S^{(*)}_8$: toggle to switch between units (counts or loss) for all IDs from 1 to 14.	$T_1 \approx$ machine run period. Calculated from ID8.
2	Loss over time T_2	s	1	$1/T_2$	sw		$T_2 \approx$months. Calculated from ID8 over last T_2 (running sum).
3	Loss over time T_3	s	1	$1/T_3$			$T_3 \approx$week(s). Calculated from ID8 over last T_3 (running sum).
4	Loss over time T_4	s	1	$1/T_4$	sw		$T_4 \approx$day(s). Calculated from ID8 over last T_4 (running sum).
5	Loss over time T_5	s	1	$1/T_5$	sw		$T_3 \approx$hour(s). Calculated from ID8 over last T_5 (running sum).
6	Loss over time T_6	s	1	$1/T_6$	sw		$T_6 \approx$minute(s). Calculated from ID8 over last T_6 (running sum).
7	Loss over time T_7	s	1	$1/T_7$	sw		$T_7 \approx$second(s). Calculated from ID8 over last T_7 (running sum).
8	Loss over pulse	s	1	$1/T_{RP}$	fw	• $S^{(*)}_8$	$1/T_{RP}$=machine repetition rate (14 Hz). Calculated over last T_{RP} (running sum).
9	Loss over BEAM_ON period	s	1	after each BEAM_ON period	fw		Only beam qualified pulses included.
10	Loss over BEAM_ON period per sent proton	s	1	after each BEAM_ON period	fw		Only beam qualified pulses included. Requires info from BCM PV(s).

Table 7 – continued from previous page

ID	Description	Type	Num. of el.	Update rate	Source	User settings	Comment
	Loss time structure in 4 different time windows inside the pulse.						
11	Loss waveform inside time window (a)	w	≤ 100	after each BEAM_ON period	fw	• $S_{9,\ldots,12}$: number of points. • $S_{13,\ldots,16}$: waveform position inside the time window with respect to a certain marker (like BEAM ON or RF ON). • $S_{17,\ldots,20}$: enable/disable monitoring (only displaying, not calculation or PV update) • $S_8^{(*)}$	Like neutron counts, the waveform is sampled at 1 MHz. Time windows: • (a): before BEAM ON and RF ON. • (b): between RF ON start and BEAM on start. • (c): inside BEAM ON. • (d): between BEAM ON end and RF ON end.
12	Loss waveform inside time window (b)	w	≤ 100	after each BEAM_ON period	fw		
13	Loss waveform inside time window (c)	w	≤ 100	after each BEAM_ON period	fw		
14	Loss waveform inside time window (d)	w	≤ 100	after each BEAM_ON period	fw		
	Scalars extracted from each of the waveforms in ID11–14						
15–18	Average losses inside windows (a,b,c,d)	s	1	after each BEAM_ON period	sw	Settings tide to settings in ID11–14, $S_{8,..,20}$	Calculated from ID11–14.
19–22	Var of losses inside windows (a,b,c,d)	s	1	after each BEAM_ON period	sw		$\mathrm{Var}(x_i) = \sqrt{(\langle x_i^2 \rangle - \langle x_i \rangle^2)}$ – variance. Calculated from ID11–14.
23–26	Min loss values in windows (a,b,c,d)	s	1	after each BEAM_ON period	sw		Calculated from ID11–14.
27–30	Max loss values in windows (a,b,c,d)	s	1	after each BEAM_ON period	sw		Calculated from ID11–14.

Table 7 – continued from previous page

ID	Description	Type	Num. of el.	Update rate	Source	User settings	Comment
	Statistic on counts and deposited charge						
31–34	Average, Var, Min and Max for neutron counts per µs	s	1	after each BEAM_ON period	fw		Calculated over BEAM_ON period.
35–38	Average, Var, Min and Max for charge in neutron events µs	s	1	after each BEAM_ON period	sw		Calculated over BEAM_ON period. Extracted from ID31–34 with $\langle \mathrm{Q\_TOT}_{1n} \rangle$ (neutron det. algorithm setting, see section 6.2.3).
39–42	Average, Var, Min and Max for charge in background events µs	s	1	after each BEAM_ON period	fw		See section 6.2.3.1 for def. of background event. Calculated over BEAM_ON period.
43–46	Average, Var, Min and Max for total charge per µs	s	1	after each BEAM_ON period	sw		Calculated over BEAM_ON period.
	Protection function block outputs - for given AMC						
47	BEAM_PERMIT	s	1	on BEAM_PERMIT change	fw		Any given AMC has one BEAM_PERMIT associated to it.
48	BEAM_PERMIT time stamp	s	1	on BEAM_PERMIT change	fw		Time stamp of BEAM_PERMIT change in ID43.
49	READY	s	1	on READY change	fw		Any given AMC has one READY associated to it.
50	READY time stamp	s	1	on READY change	fw		Reports time stamp of current READY value from ID45 .
51	Protection algo	s	1	on algo selection change	fw		Indicates which protection algorithm is currently selected for BEAM_PERMIT calculation.

Table 7 – continued from previous page

ID	Description	Type	Num. of el.	Update rate	Source	User settings	Comment
	Same as ID11–30 but for Protection function relaxation filter output.						
52–55	Waveform in 4 time windows	w	as in ID11-14	after each BEAM_ON period	fw	$S_{9,..,20}$ – as in ID11–14.	
56–71	Statistics in 4 time windows	s	1	after each BEAM_ON period	fw	$S_{9,..,20}$ – as in ID15–30.	
	Same as ID11–30 but for Protection function X/Y algorithm output.						
72–75	Waveform in 4 time windows	w	as in ID11-14	after each BEAM_ON period	fw	$S_{9,..,20}$ – as in ID11–14.	
76–91	Statistics in 4 time windows	s	1	after each BEAM_ON period	fw	$S_{9,..,20}$ – as in ID15–30.	
	Same as ID11–30 but for Protection function Moving Average filter output for time constant $t_{MA,1}$.						
92–95	Waveform in 4 time windows	w	as in ID11-14	after each BEAM_ON period	fw	$S_{9,..,20}$ – as in ID11–14.	
96–111	Statistics in 4 time windows	s	1	after each BEAM_ON period	fw	$S_{9,..,20}$ – as in ID15–30.	
	Same as ID11–30 but for Protection function Moving Average filter output for time constant $t_{MA,2}$.						
112–115	Waveform in 4 time windows	w	as in ID11-14	after each BEAM_ON period	fw	$S_{9,..,20}$ – as in ID11–14.	
116–131	Statistics in 4 time windows	s	1	after each BEAM_ON period	fw	$S_{9,..,20}$ – as in ID15–30.	

Table 7 – continued from previous page

ID	Description	Type	Num. of el.	Update rate	Source	User settings	Comment
	Detector specific data						
132	Pedestal	s	1	$1/T_{RP}$	fw	• S_{21}: Time window length or number of points for pedestal cal. • S_{22}: Position of time window inside the pulse. • $S_{23}^{(*)}$: Toggle to indicate if samples inside events should be excluded.	Raw data must be used for pedestal calculation. The window should be placed before the BEAM ON period.
153	Noise (pedestal variance)	s	1	$1/T_{RP}$	fw		Calculated with the same data sample as pedestal.
134	Number of pos. ADC saturations per pulse	s	1	$1/T_{RP}$	fw		Summed over T_{RP}.
135	Number of neg. ADC saturations per pulse	s	1	$1/T_{RP}$	fw		Summed over T_{RP}.
	`EventInfo` statistic: single neutron events						
136–139	Average, Var, min and max for $\texttt{Q\_TOT}_j$	s	1	every $N_{e,1}$ events	fw	$S_{24} = N_{e,1}$: number of single neutron events	Calculated with $N_{e,1}$ successive events identified as single neutrons which were not split at the edge of MTW ($\texttt{isTruncated}_j = \texttt{false}$ $\texttt{isPart2}_j = \texttt{false}$ – see section 6.2.3). Time stamp indicating the origin of data is also available.
140–143	Average, Var, min and max for $\texttt{peakValue}_j$	s	1	every $N_{e,1}$ events	fw		
144–147	Average, Var, min and max for $\texttt{TOT}_j$	s	1	every $N_{e,1}$ events	fw		
148–151	Average, Var, min and max for $\texttt{riseTime}_j$	s	1	every $N_{e,1}$ events	fw		
	Other information						
152	AMC health status	s	1	$1/T_{RP}$	fw		Last value of the AMC health status.
153	Smart Trigger condition status	s	1	on change	fw		Indicates if the condition to issue the conditional DoD trigger request has been met on a given AMC.

8 Startup procedure and system commissioning

All verification tests and procedures planned to be performed during system commissioning with or without beam are detailed in [38]. In addition to this the document specifies all the tests that are planed for parts of the system or as a whole before and after the installation. Here only a short summary of the strategy for the system commissioning is given.

The following is planned to be configured during the nBLM system commissioning:

- **Pedestal setting**
  The value must be set before all other settings. It is configured for each detector separately in two ways:
  - By checking the pedestal value monitored on the firmware level (ID132 in table 7).
  - By histogramming the raw data extracted through the DoD feature.

  Note that no beam is required to tune this setting.

- **Neutron algorithm settings**
  To increase the statistic of detected neutrons, controlled losses are planed to be used to tune these values. The DoD feature is used to extract event amplitude and TOT together with rise time and charge distributions from either raw data or `EventInfo` data stream. The distributions serve as a guide to select the algorithm settings. Note that the settings must be tuned for each detector separately.

- **Trigger delay**
  For each detector the delay with respect to the 14Hz triggers distributed by the timing master (EVG – Event Generator) needs to be configured to account for difference in cable lengths and potentially detector locations. This can be performed by monitoring accumulated loss over beam pulse (see ID9 in table 7). For each trigger delay setting an average value for the loss accumulated over beam pulse is extracted. Here the beam pulse refers to the time period with BEAM_ON. The best trigger setting gives the highest average value for the accumulated loss.
  The test requires beam present. It should be repeated after each cable length change which includes connecting a detector to a different digitiser channel or AMC card.

- **Verification of Monte Carlo (MC) simulations and equivalent loss scaling factor.**
  A set of controlled losses that are used for verification of the MC simulation geometry model needs to be identified. The simulation results are compared to the measurements performed during the commissioning. In case of larger discrepancies, the source of those is identified and simulation model modified accordingly. The process is iterative.
  Once the simulation model is verified and understood, the results are used to extract the equivalent loss scaling factors for each detector, where each controlled loss scenario has a group of detectors assigned to. These scaling factors are used to convert measured neutron counts to the equivalent number of lost protons (see section 7.2). Note however,

that the factor is referred to equivalent due to the fact that it is extracted from one of the possible loss scenarios and is therefore in general incorrect for all other scenarios.

- **Protection algorithm commissioning**
  A set of controlled loss scenarios with different time evolution of the loss need to be identified. The scenarios as used to tune the protection algorithm through experience and simulations. The initial tuning with experience is foreseen for system commissioning. The tuning is needed whenever an unchecked change in protection algorithm is considered.

- **Machine Protection (MP) thresholds**
  A set of likely scenarios of accidental losses that are most damaging is identified. MC simulations coupled with thermo–mechanical ones are used to asses the damage potential for these scenarios. A risk matrix connecting damage potential and cost is then generated which serves as a baseline for MP threshold selection.

The system needs to have detector (channel) pre–processing (pedestal value) and neutron algorithm settings configured in order to operate correctly. The values are planned to be tuned during the system commissioning. However, they require reconfiguration each time detector settings (HV, LV or any mechanical change effecting the charge drift or multiplication) or cable length is changed. Unless learned otherwise trough the system commissioning experience, rechecking the values after longer shutdowns is not strictly required, as alarms will be present on certain monitoring values (pedestal, average neutron amplitude and charge, see table 7) to detect potential problems with the data processing settings as well as problems in the signal generation, signal amplification or data processing chain.

Similarly loss scaling factors and MP thresholds may require reconfiguring after a change in detector settings. However, it might be possible to scale their values by comparing certain variables before or after the change. The exact procedure will be developed after or during the system commissioning once the system performance is well understood.

9 Document revision history

Revision	Change	Author	Date
1	Document creation	Irena Dolenc Kittelmann	2016-02-26
2	Tech. spec. for IK annex with DEDIP	Irena Dolenc Kittelmann	2016-03-02
3.1	Adding req. and updating spec., adding data processing, monitoring and control spec.	Irena Dolenc Kittelmann	2018-07-26
3.2	Update	Irena Dolenc Kittelmann	2018-08-08
4.0	Added prot. function and Smart trigger descr.; updated monitoring chapter; added mech. support section, format change; added startup and commissioning section; other smaller updates	Irena Dolenc Kittelmann	2019-01-15

References

[1] E. Donoghue et al, *Studies of electronic activities in SNS-type SC RF cavities*,. Proc. 12th Int. Workshop on RF Superconductivity, Cornell Univ., USA, TUP67 (2005).

[2] PBI L4 requirements, ESS-0078645.

[3] A. Nordt, *Beam Instrumentation interfaces to protection systems*, TAC12, https://indico.esss.lu.se/indico/event/315/session/9/contribution/32/material/2/1.pptx.

[4] C. Amstutz, *FPGA Development Standards*, available on https://confluence.esss.lu.se/display/RFG/FPGA+Development+Standards; the following tabs are of interest in case of the BLM systems: *FPGA Coding Guidelines*, *Naming of AXI ports*, *RTL Design Libraries* and *Project Organization* – where IOxOS does not provide information.

[5] L. Tchelidze, *How Long the ESS Beam Pulse Would Start Melting Steel/Copper Accelerating Components?*, ESS/AD/0031

[6] I. Dolenc Kittelmann, *Report regarding the MC simulations for the BLM - focus on the nBLM*, August 2016, ESS-0066428

[7] https://www.ioxos.ch/produit/adc-3110-3111/

[8] https://www.ioxos.ch/produit/ifc_1410/

[9] http://www.caen.it/jsp/Template2/CaenProd.jsp?idmod=752&parent=20

[10] http://www.caen.it/jsp/Template2/CaenProd.jsp?idmod=944&parent=20

[11] http://www.caen.it/jsp/Template2/CaenProd.jsp?idmod=875&parent=20

[12] https://www.siemens.com/global/en/home/products/automation/systems/industrial/plc/simatic-s7-1500.html

[13] L. Segui, *nBLM Gas System: Pipes specifications*, 2nd version, August 2018, available on https://confluence.esss.lu.se/display/BIG/BLM+documents (document nBLM_GasPipes_v2_withPIDs.pdf); also available as part of nBLM CDR3 documentation on https://indico.esss.lu.se/event/1173/

[14] https://confluence.esss.lu.se/display/BIG/BLM+documents, document by L. Segui, (distributionGas_detector_option2_Feb2018.xlsx).

[15] I. Dolenc Kittelmann, *"Report regarding the MC simulations for the BLM - focus on the nBLM"*, August 2016, ESS-0066428

[16] I. Dolenc Kittelmann, T. Shea, *Simulations and Detector Technologies for the Beam Loss Monitoring System at the ESS linac*, HB2016, THAM6Y01, 3.-8. July, 2016, Malmö, Sweden.

[17] L. Segui, *nBLM project – PDR1.1*, report for nBLM PDR1, Dec. 2016, ESS-0087794, also available on https://indico.esss.lu.se/event/735/

[18] L. Segui, *Monte Carlo results: nBLM response to ESS scenarios*, report for nBLM PDR2, July 2017, ESS-0107320, available on https://indico.esss.lu.se/event/835/

[19] *nBLM system – PDR1.2*, report for nBLM PDR2, July 2017, ESS-0513009, available on https://indico.esss.lu.se/event/835/

[20] L. Segui, *Modes covered by nBLM system*, report for nBLM CDR1, Dec. 2017, ESS–0324205, available on https://indico.esss.lu.se/event/948/

[21] P. Legou, *Beam Spectrometers using Micromegas in Time projection Chamber mode*, HB06, Tsukuba, Japan, 2006, WEBZ03.

[22] L. Segui, *ESS nBLM system: Detector design and materials selection for 84 deliverable detectors production*, report for nBLM CDR2, July 2018, ESS-0513258, available on *https://indico.esss.lu.se/event/1083/*

[23] L. Segui, *nBLM detectors experimental results*, presentation at nBLM CDR2, 12. July 2018, ESS-0513259, available on *https://indico.esss.lu.se/event/1083/*

[24] L. Segui, *nBLM project – CDR1.1*, report for nBLM CDR1, Dec. 2017, ESS-0324206, available on https://indico.esss.lu.se/event/948/

[25] P. Legou, *nBLM Front-End Electronics*, presentation at nBLM CDR1, Dec. 2017, ESS-0324199, available on https://indico.esss.lu.se/event/948/

[26] I. Giomatris, *Development and prospects of the new gaseous detector Micromegas*, NIMA, vol. 419, p.239, 1998.

[27] I. Giomatris et al, *Micromegas in bulk*, NIMA, vo. 560, p.405, 2006

[28] I. Dolenc Kittelmann, https://jira.esss.lu.se/browse/BIG-1248

[29] H. Kočevar, *Data on demand feature*, July 2018, available on https://indico.esss.lu.se/event/1073/

[30] I. Dolenc Kittelmann, *nBLM: Neutron Detection Algo*, nBLM meeting, 10–11. July 2018, ESS, Lund, Sweden; available on https://indico.esss.lu.se/event/1073/

[31] Y. Mariette et al, *nBLM Control System Design*, report and presentation at nBLM CDR3, available on https://indico.esss.lu.se/event/1173/,

[32] I. Dolenc Kittelmann, *nBLM: Circular Buffers*, nBLM meeting, May 2018, available on https://confluence.esss.lu.se/display/BIG/2018-05-30+meeting+with+DMCS

[33] I. Dolenc Kittelmann, *Block digram of nBLM functinality*, https://jira.esss.lu.se/browse/BIG-1151

[34] I. Dolenc Kittelmann, https://bitbucket.org/europeanspallationsource/nblm-fw-simtools/src/default/

[35] I. Dolenc Kittelmann, https://bitbucket.org/europeanspallationsource/nblm-fw-testtools/src/default/

[36] L. Segui, *nBLM project CDR1.2 – final*, report for nBLM CDR3, Feb. 2019, available on https://indico.esss.lu.se/event/1173/

[37] G. Jablonski et al, *nBLM firmware implementation*, report and presentation at nBLM CDR3, available on https://indico.esss.lu.se/event/1173/

[38] C. Derrez, C. Lahonde-Hamdoun, *nBLM verification plan*, report and presentation at nBLM CDR3, available on https://indico.esss.lu.se/event/1173/

[39] Q. Bertrand, *Gas rack design and gas components*, presentation at nBLM CDR2, 12. July 2018, available on *https://indico.esss.lu.se/event/1083/*

[40] Q. Bertrand, *Gas box design, ESS nBLM, version 1.0*, report for nBLM CDR2, 12. July 2018, available on *https://indico.esss.lu.se/event/1083/*

[41] T. Papaevangelou, *ESS nBLM system: Detector design review*, presentation at nBLM CDR2, 12. July 2018, ESS-0513258, available on *https://indico.esss.lu.se/event/1083/*

[42] L. Segui, *nBLM project – reort, Experimental Tests, CDR12 final*, report for nBLM CDR3, Feb. 2019, available on https://indico.esss.lu.se/event/1173/

[43] E. Bergman, P. Legou, *nBLM FEE and cables*, presentation at nBLM CDR3, Feb. 2019, available on https://indico.esss.lu.se/event/1173/

[44] *ICD between BLMs and the FBIS*,ESS–0515969, also availale on https://indico.esss.lu.se/event/1173/